NASA Contractor Report 3929

Studies on Effects of Boundary Conditions in Confined Turbulent Flow Predictions

M. Nallasamy and C. P. Chen

NASA

NASA Contractor Report 3929

Studies on Effects of Boundary Conditions in Confined Turbulent Flow Predictions

M. Nallasamy and C. P. Chen
Universities Space Research Association
Columbia, Maryland

NASA

National Aeronautics
and Space Administration

**Scientific and Technical
Information Branch**

1985

TABLE OF CONTENTS

iii

LIST OF ILLUSTRATIONS

I. INTRODUCTION

Two equation turbulence models used in the computation of the turbulent flows involve the specification of five or six constants. These constants have been evaluated using the experimental data on boundary layer flows. These are not changed during any calculation. However, these are not universal constants. They need to be changed for predictions of different classes of flows, for example predictions of plane two-dimensional jet and axisymmetric jet [1,2] The constants have to be changed to correctly predict the spread rate of an axisymmetric jet. The constants have to be changed in order to accommodate the effects such as streamline curvature, low Reynolds number, near wall region, etc. [3]

Another important element in the predictions is the specification of inlet boundary conditions. Sometimes they are considered of minor importance while evaluating the performance of turbulence models against experimental data. Assumed boundary conditions can lead to wrong conclusions about the performance of the model [3,4]. In particular, the inlet profiles of **k** and e can have a significant effect on the flow downstream. The profiles of **k** may be evaluated from the experimental data. But no satisfactory method of evaluating the inlet profile of E **is** available The inlet conditions become more controlling when the inlet flow has a swirl component. For example, only with a "suitable" initial condition, can the coswirl flow in coaxial jets be predicted [5] In addition, minor changes in the E level of the inlet section have been found to have the same degree of modifications on the flow field as the swirl related corrections to the turbulence model [6]

In the case of complex flow configurations, such as the SSME internal flow configuration, it is not expected that detailed inlet boundary conditions will be available from experimental measurements. In such cases it is important to include a sensitivity test to the initial conditions in turbulence model predictions. The issue of initial conditions is more important in internal flows, where elliptic procedures are used for the numerical solutions, than the free shear flows or boundary layer type flows, where parabolic, marching techniques are employed. In boundary layer type flows, the evaluation of the physical turbulence model is always made in the self preserving region, where the influence of the inlet condition is insignificant [7] In internal flows, especially flows with recirculation, the influence of the inlet boundary conditions may extend up to the reattachment point.

In this report an effort is made to understand the difference in **k-e** model predictions of confined plane two-dimensional expansion flow, and axisymmetric sudden expansion flow. Model constants are not changed to correctly predict the experimental data. Only the predictions for the same initial flow conditions and expansion ratio are examined. The predicted results of the flow over a backward-facing step, the symmetric plane two-dimensional expansion flow, and the axisymmetric expansion flow are compared. The report also presents the calculations **of** the flow in a confined coaxial jet. The predictions of the coaxial jet with the velocity ratio of annulus to central jet, equal to unity are compared with those of an axisymmetric sudden expansion flow. Results are also presented for different ratios of annulus to central jet velocities.

The effects of inlet k-e profiles and Reynolds number on the predicated reattached lengths in the case of axisymmetric expansion are investigated, The effects of inlet turbulence level are significant for the case of confined coaxial jet in which the development of the flow is highly dominated by the coupled diffusion processes and the interactions of the incoming annular and central jet flows. The situation is more complicated when the inlet swirl is present in the annular region where the diffusion process is coupled with the extra strain induced by the streamline curvature. *An* effort is also made to investigate the sensitivity of the inlet turbulence level on the swirling flow field.

The predictions reported here have been carried out using PHOENICS [8] and TEACH [9] codes. These codes use in principle the same form of the equations governing the flow [10] However, they differ in the details of the solution procedures. A comparison of the prediction of the two codes for the axisymmetric sudden expansion flow is presented.

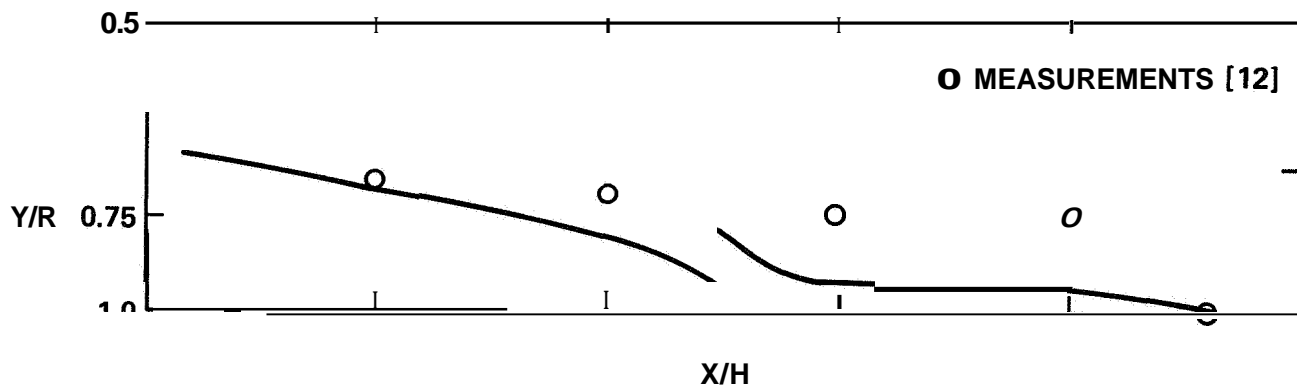## II. PLANE TWO-DIMENSIONAL AND AXISYMMETRIC RECIRCULATING FLOWS

The k-ϵ turbulence model is used in a majority of all turbulent flow predictions, The standard model uses five constants determined for boundary layer flows. These constants are not as universal as one expects them to be. For example, the standard model predicts the spread rate of a plane jet correctly while it overpredicts the spread rate of a circular jet, Several modifications of the model have been proposed for improving the prediction of circular jets [1]. However, no modification of the model produces correct predictions for all axisymmetric and plane two-dimensional cases [2].

A close examination of the confined recirculating flows seems to indicate that such anomaly between the plane two-dimensional **and** axisymmetric predictions is present in the computations of internal flows as well. Specifically, the length of the recirculation region, X_r is underpredicted by about 20 percent for the flow over a backward-facing step, whereas X_r for an axisymmetric sudden expansion is predicted within the expenmental accuracy. The reattachment lengths reported by several investigators for backward-facing step and axisymmetric expansion, respectively, illustrate the point [31 The poor performance of the k-e model for the backward-facing step flow is not clear,

A specific comparison of the prediction of the recirculation region for the two cases with measured data is shown in Figure 1. In Figure 1a, the length of the recirculation region **is** predicted accurately for the pipe expansion [12,131 The figure shows the locus of the flow reversal ($\overline{U} = 0$). The flow reversal line shown for the backward-facing step (Fig. 1b) shows the rather severe underprediction of the separation length [11] In both cases the width of the recirculation region is not very well predicted.

A. Boundary Condition Effects

In this report, an effort is made to explain the differences in predictions of plane and axisymmetric-confined recirculating flows. The flow over a backward-facing step, the flow in a plane symmetric expansion, **and** the flow in an axisymmetric pipe expansion are computed for the same inlet conditions. The Reynolds number based on the upstream channel width (diameter) **is** 9.3 x 10^4 A grid of 42 x 42 is used to produce grid independent solutions. The expansion ratio **is** 1.5 for which experimental data for backward-facing step flow is available.

2

0.5

O MEASUREMENTS [12]

Y/R   0.75

1.0

X/H

(a) Axisymmetric expansion.

Y/H
1.0

O   EXPERIMENT [11]
── PREDICTION

0.5

REATTACHMENT

POINT

0

2   4   6   8

X/H
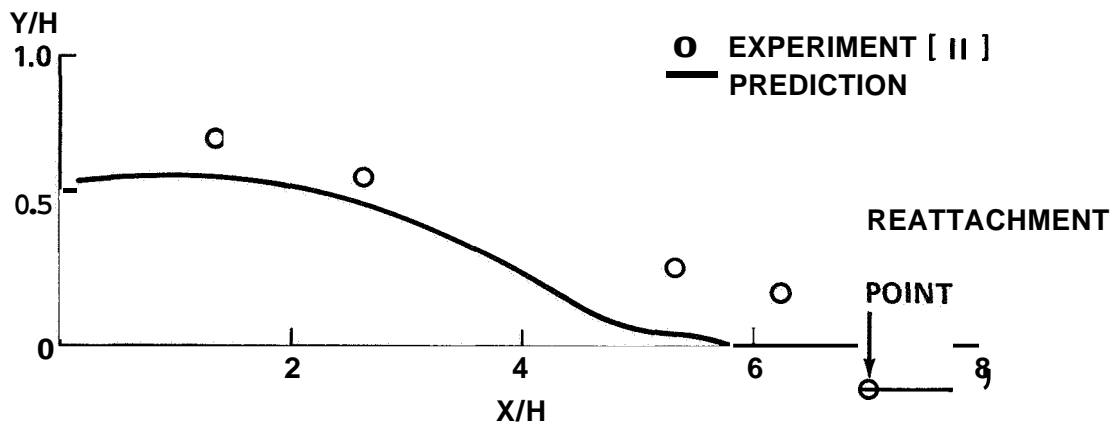
(b) Backward-facing step.

Figure 1, Locus of flow reversal.

1   The Keattachment Length

The single most important parameter to compare in these flows is the reattachment length X_r.
The reattachment length for the backward-facing step is obtained as 5.8H as compared to the "accepted" experimental value of 7H [11], where H is the step height.   The X_r for the pipe expansion is 7 7H for this expansion ratio.   The symemtric two-dimensional expansion has an intermediate value of 6.3H.
The reduction of X_r from 6.3H for symmetric expansion to 5.8H for the asymmetric expansion is due to the stabilizing effect of the presence of the top wall instead of a symmetry line.   The effect is not very significant in this case but has been found to be significant in the case of bluff body stabilized flows [14].   Now, consider only the plane two-dimensional symmetric expansion and axisymmetric expansion.   In the limiting case of walls at infinity, free shear flow, the spread rate of the plane-separated layer is higher than the axisymmetric one, as shown by the experiments.   For the finite step height the initial shear layer is unaware of the wall and thus the spread rates follow more or less the same trend as in the unconfined flows.   Thus, for the plane symmetric expansion, X_r is shorter than that for the axisymmetric expansion.

a

a. Mean Velocity Profiles

Prediction of the flow over a backward-facing step was studied extensively in the 1980-81 Stanford conference on complex turbulent flows. The mean velocity profiles behind the step at three different downstream distances obtained in the present study are shown in Figure 2. The experimental data for the backward-facing step and the predictions for plane symmetric expansion and the axisymmetric expansion are also shown in the figure. It is seen that the mean velocity profile in the separated region is predicted inaccurately. This seems to stem from the wall function used. Because of the nature of implementation of the wall function used, the first point next to the wall has the hghest return flow velocity, in all the computations. This is not true in the actual flow. The way of handling the wall function in the PHOENICS code appears to result in a peaked mean velocity from the near-wall node point to the subsequent points [15] This is discussed in Section IV
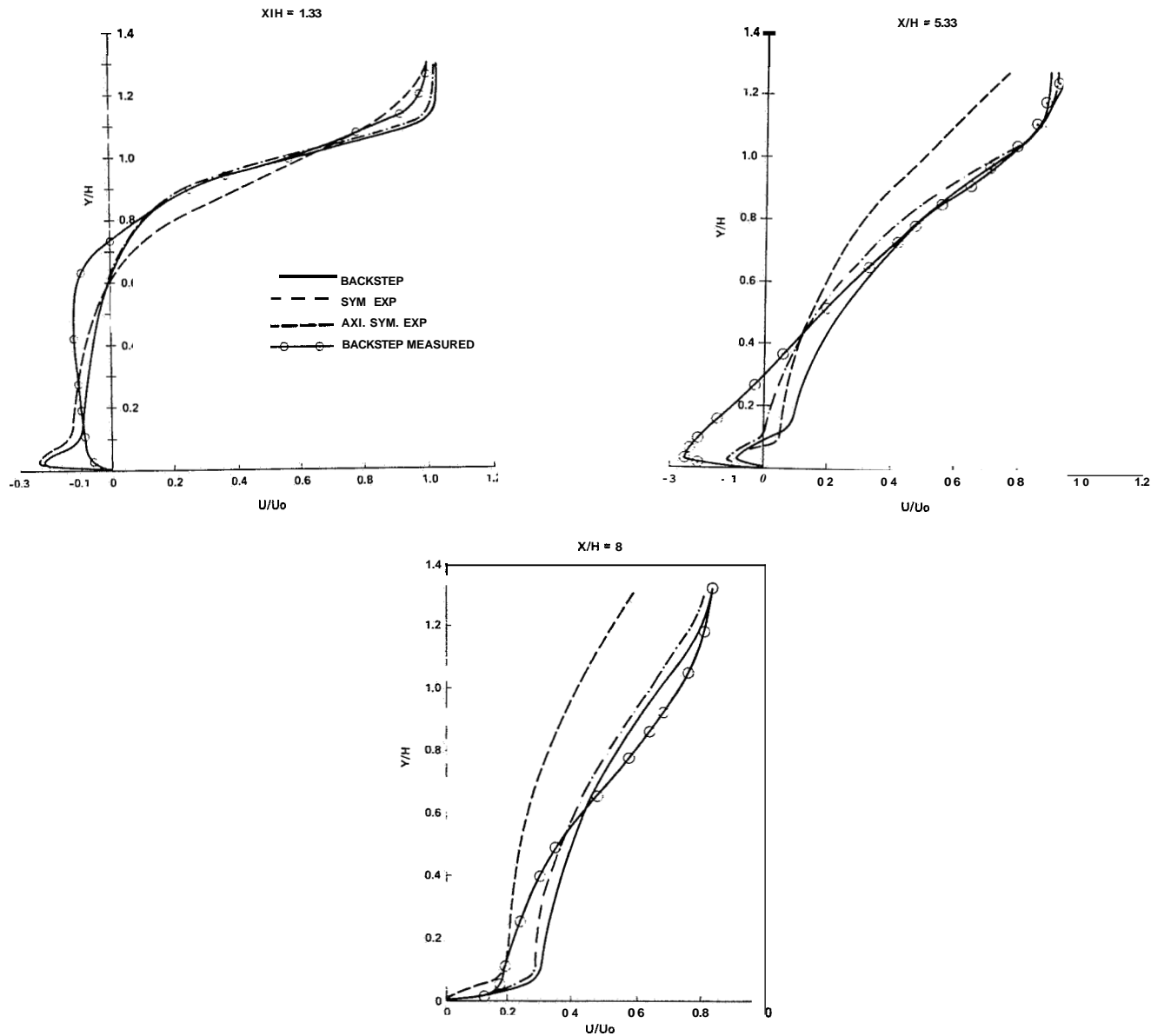

Figure 2. Mean velocity profiles (X/H = 1.33, 5.33, 8.0).

4

The mean velocity profile predictions for the plane symmetric expansion and the flow over a backward-facing step show more or less a similar trend. In the axisymmetric expansion case, the flow (development) expansion is slower as shown by the mean velocity profiles (Fig. 2a-2c). This is also seen in the variation of the centerline velocity in the streamwise direction (Fig. 3). In the region just downstream of the expansion, the decay rate of the centerline velocity is substantially higher for plane symmetric expansion, for a higher expansion ratio of 2 (Fig. 3b). The experimental data of Reference 12 for the pipe expansion are also shown. The prediction is in fairly good agreement with the measurements. The faster decay of the centerline velocity in the plane flow causes a stronger streamline curvature than with the axisymmetric case. The computation of the production term in the ε-equation

$$P = -\overline{u_i u_j} \frac{\partial U_i}{\partial x_j}$$

tends to be more inaccurate in the plane expansion. For this reason, even the correction of the production and dissipation terms in the ε-equation for the k-e model does not improve its performance for the plane flow. The algebraic stress model employing an algebraic equation for $\overline{u_i u_j}$, can only improve the prediction of the two-dimensional expansion [15,30].
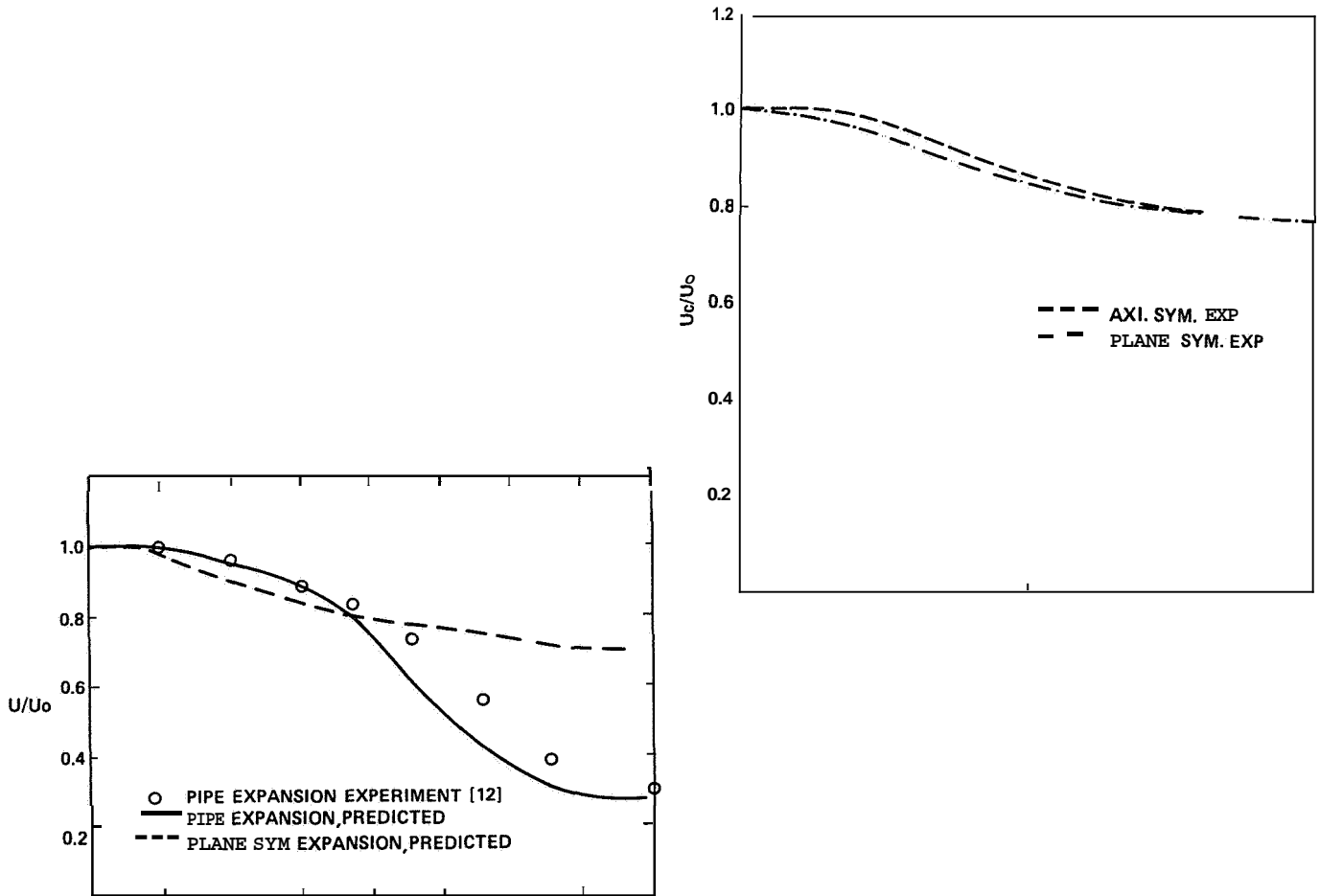

Figure **3.** Variation of centerline velocity.

b. Kinetic Energy

The kinetic energy profiles just downstream of the expansion are shown for the three cases in Figure 4. For all the three cases, the profiles show the characteristics of the separated region. That **is,** just downstream of the expansion, the kinetic energy maximum occurs in the separated layer at a y/H of 1.0. Further downstream of the expansion, the location of the kinetic energy maximum moves closer to the wall, as in the attached flows. However, the kinetic energy level is higher for the axisymmetric expansion than for the plane expansion flow, The kinetic energy contours in the entire computational field are shown in Figure 5 for the three cases, for an expansion ratio of 1.5. Figure *6* shows the contours for an expansion ratio of **2.** For this expansion ratio the contours for the backward-facing step and the symmetric expansion are similar, except that the symmetric case shows a slightly shorter core region. The contours for the axisymmetric expansion clearly show a shorter core region as compared to the plane flow **This** is in accordance with the experimental observations [17]. Also, as observed in the experiments, the core region extends beyond the reattachment point in the plane flow, while in the axisymmetric flow the opposite holds (Fig. **7).**
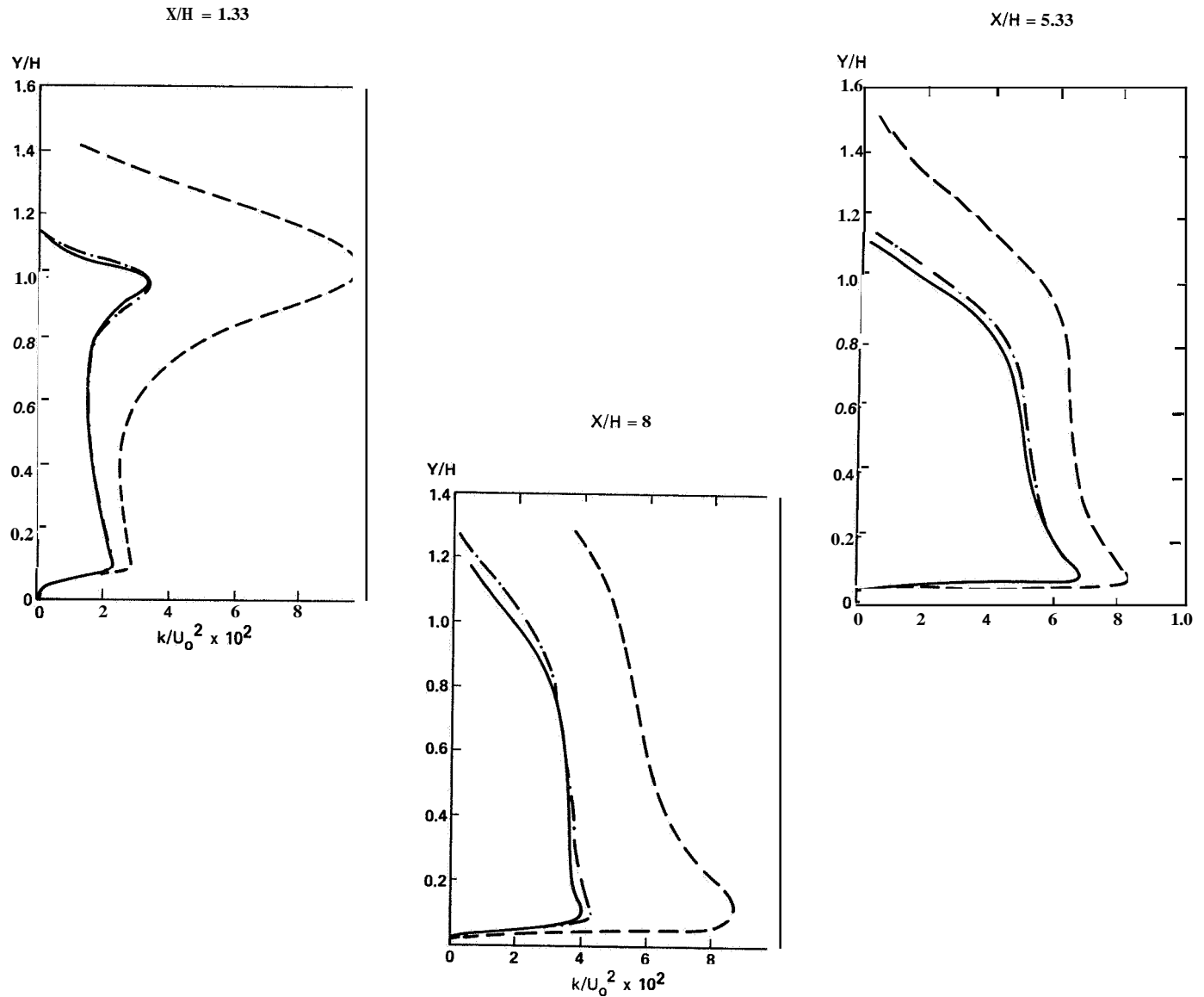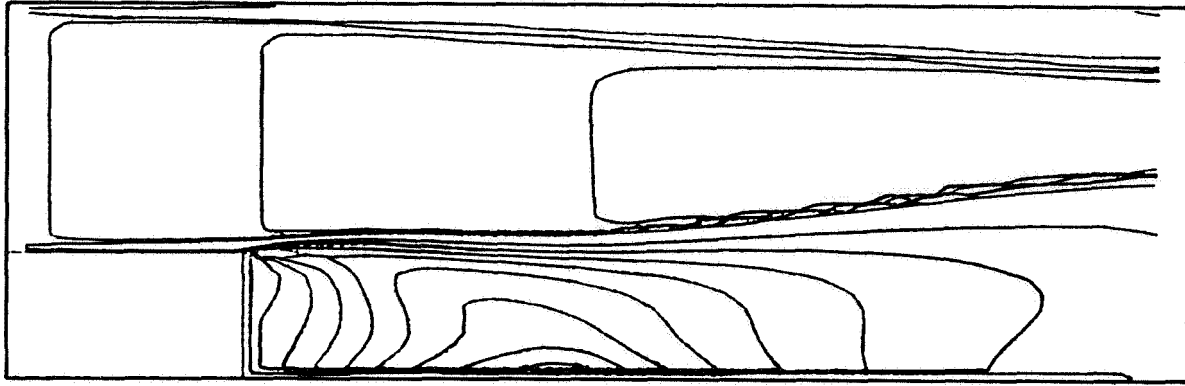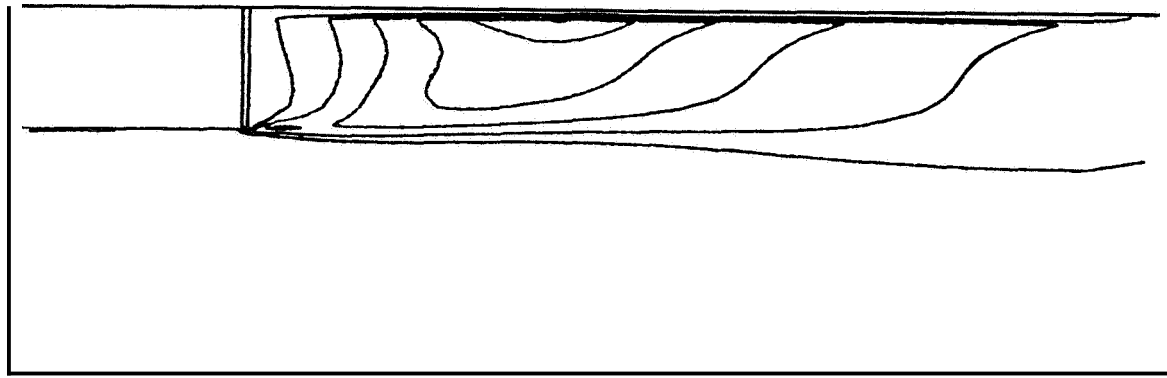

Figure 4. Kinetic energy profiles (X/H = 1.33, **5.33,** 8.0).

(a) Backward-facing step.

(b) Plane symmetric expansion.
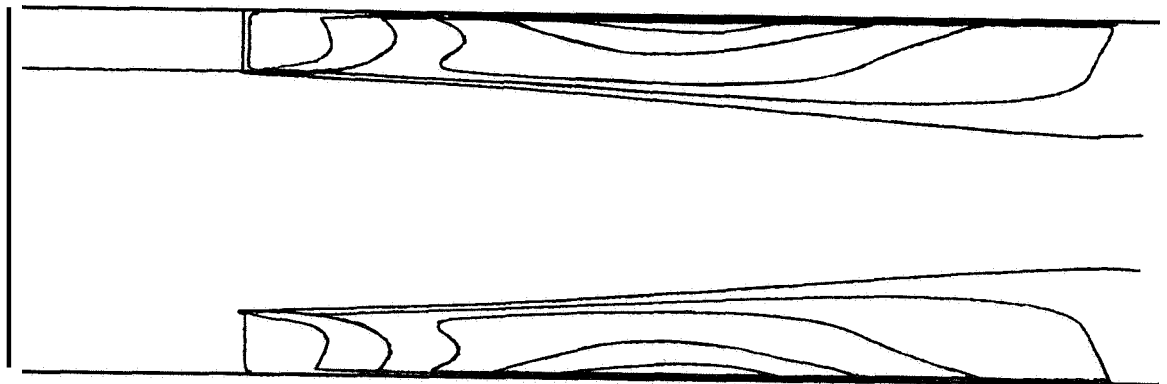
(c) Axisymmetric expansion.

Figure 5   Contours of kinetic energy (expansion ratio = 1.5).
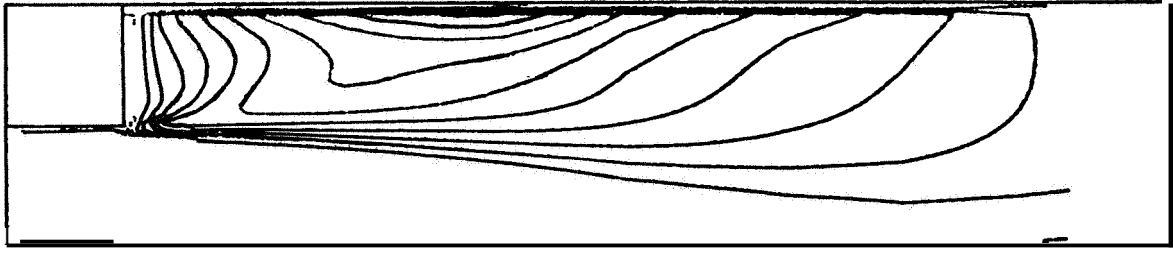
(a) Backward-facing step.
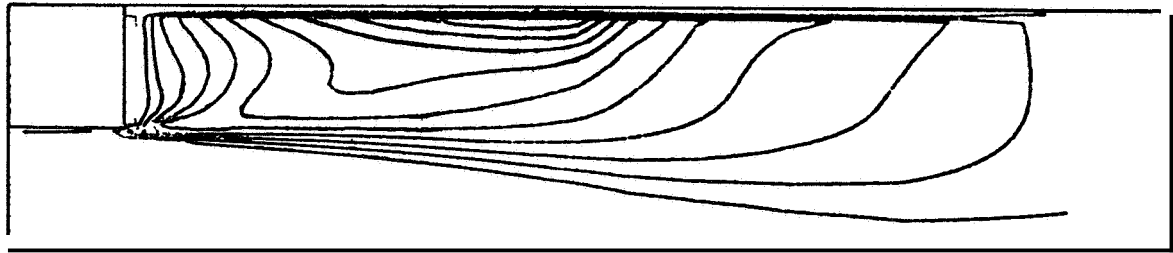
(b) Plane symmetric expansion.
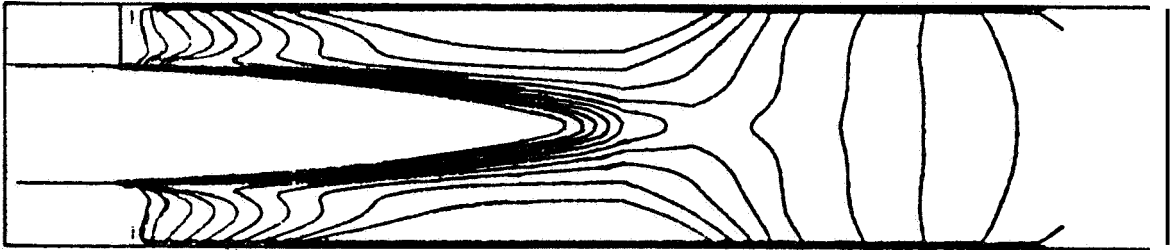
(c) Axisymmetric expansion.

Figure 6. Contours of kinetic energy (expansion ratio = 2.0).

c. Dissipation Rate of Kinetic Energy

The kinetic energy dissipation rate profiles for an expansion ratio of 2 are shown in Figure 8. **As** for the kinetic energy, the dissipation rate contours for the backward-facing step and the symmetric plane expansion are similar. However, the contours for the axisymmetric case show the short-core region.

d. Wall Static Pressure Variation

The wall static pressure variations for the three cases for an expansion ratio of 1 5 are shown in Figure 9 The pressure recovery downstream of the reattachment is faster in the case of plane two-dimensional expansions compared to the axisymmetric case. This is consistent with the shorter reattachment lengths predicted for plane flow

8
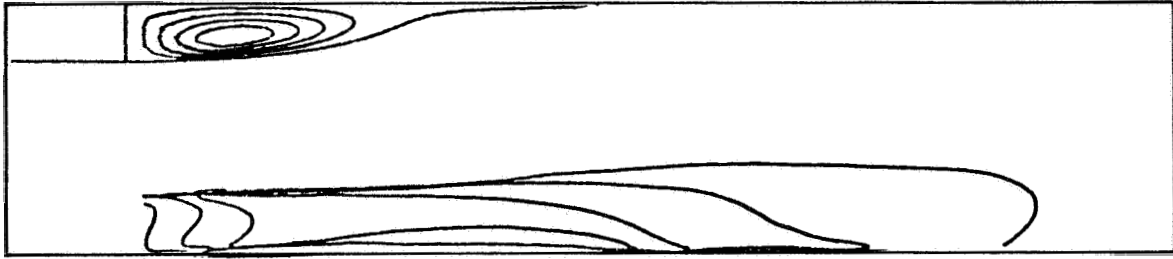
(a) Plane symmetric expansion.
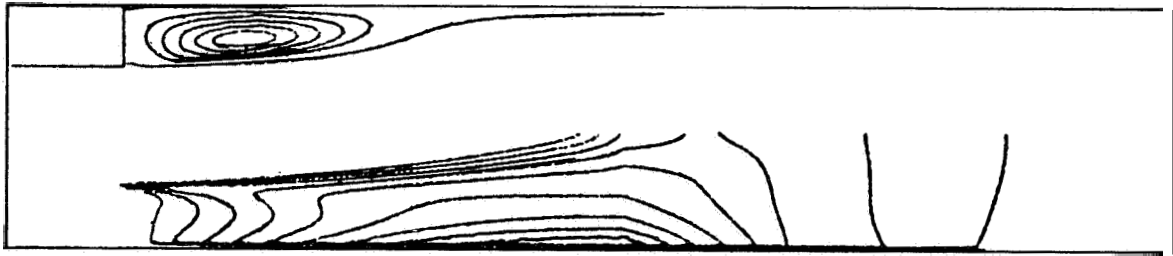
(b) Axisymmetric expansion

Figure 7. Core region **and** recirculation region.
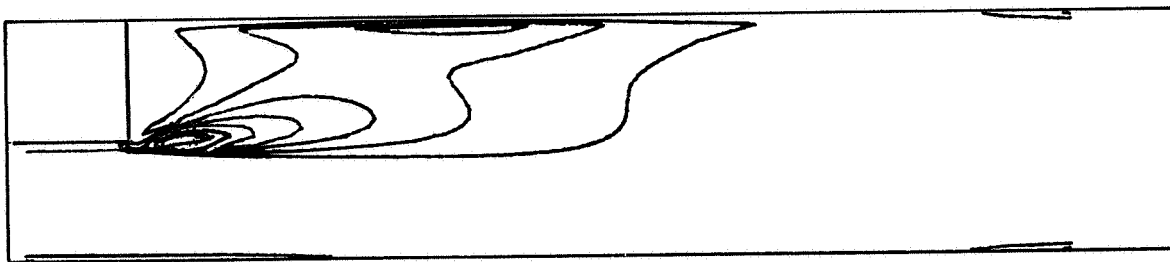
(a) Backward-facing step.
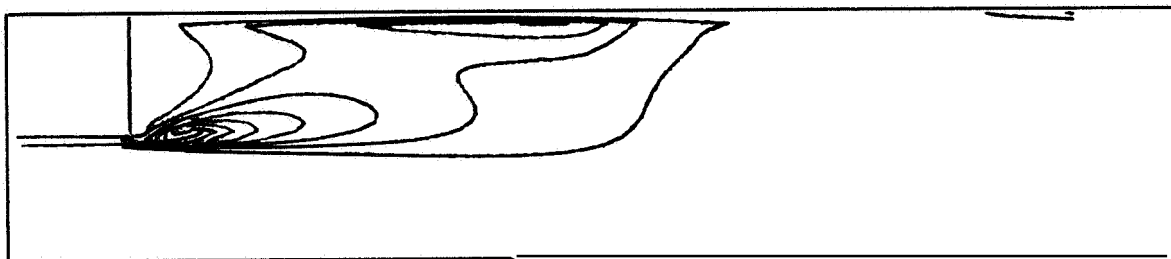
(b) Plane symmetric expansion,
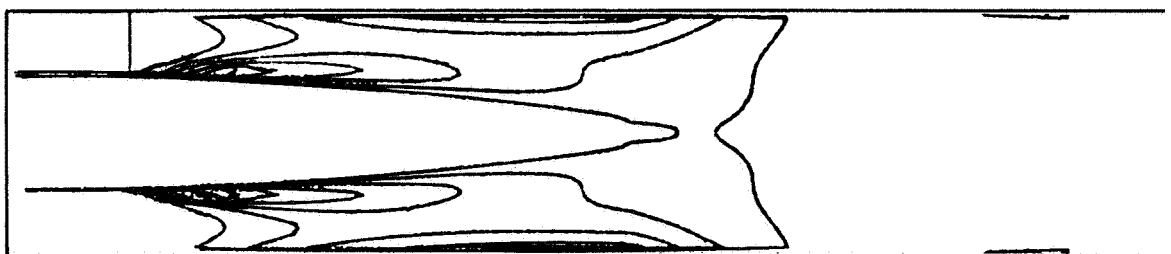
(c) Axisymmetric expansion.

Figure **8.** e-profiles for expansion ratio **=** 2.0.
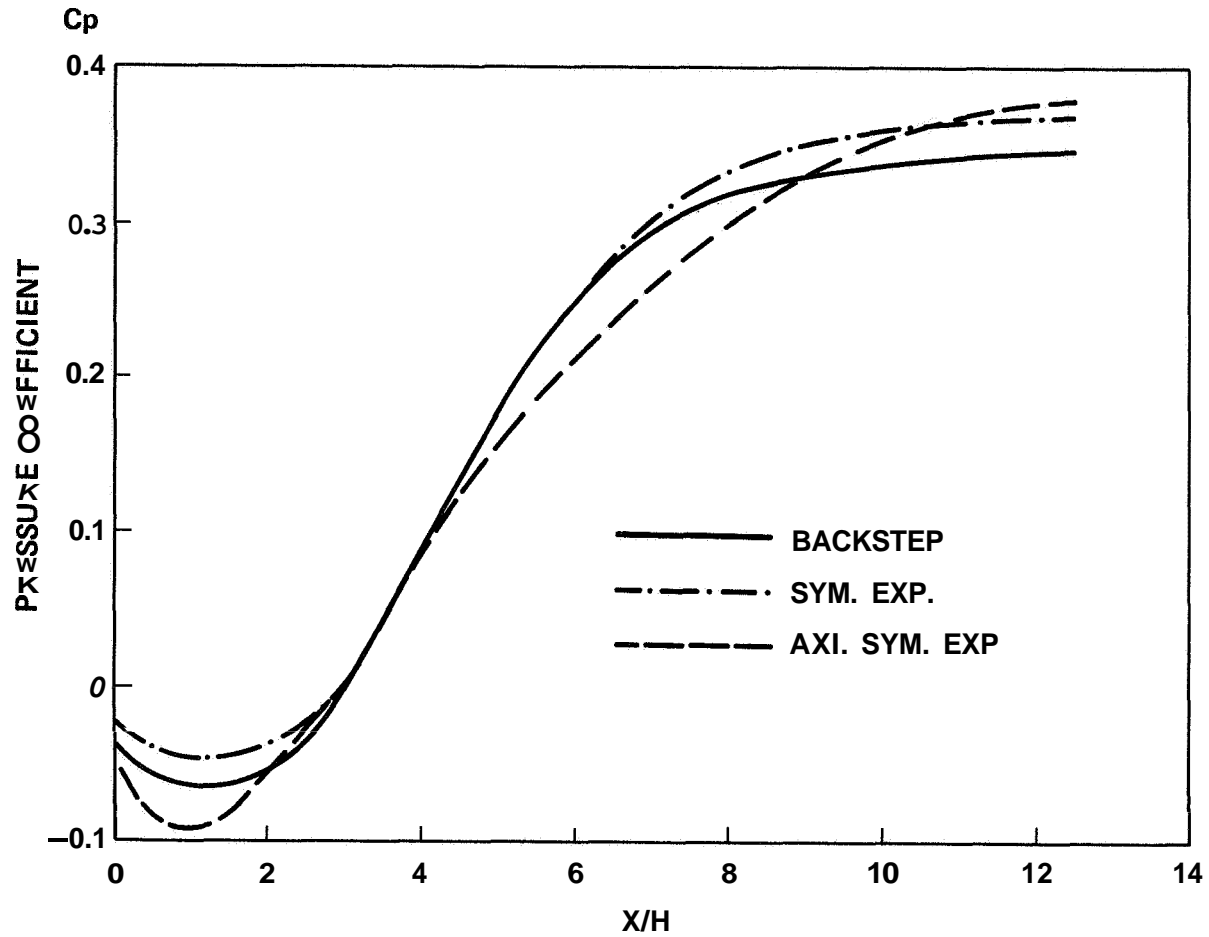
Figure **9.** Wall static pressure distributions.

B. Sensitivity of the Axisymmetric Expansion Flow to Inlet Boundary Conditions

The inlet mean velocity profile **is** normally available from the measurements. Otherwise, either a fully developed flow or a plug flow is specified in the predictions. Measurements show that a thicker inlet boundary layer produces a larger recirculation region [30]. However, the predictions show only a small increase in X_r (about 2 percent) for the fully developed flow as compared to plug flow

The specification of inlet profiles for k and ϵ **is** more difficult. The **k** profile may be estimated from the measurements. In general, **k is** specified as a percentage of the inlet mean square velocity

$$k_{in} = 0.003 \times U_{in}^2 \tag{1}$$

Depending on the percentage (constant), the predicted results vary. For example the reattachment length X_r can vary as much as 1.0H as shown in Figure 10, by varying the constant,

11
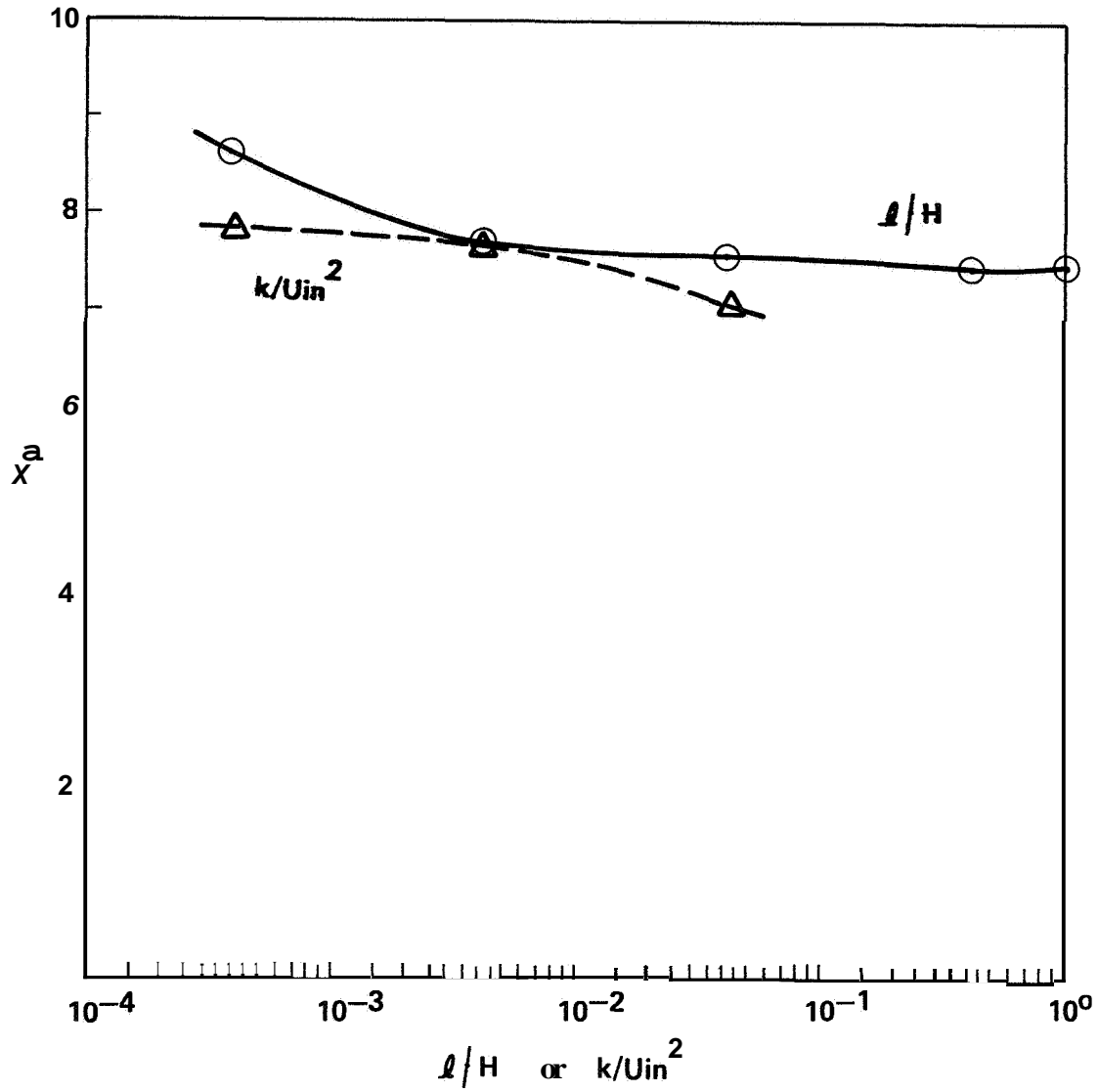
Figure 10. Variation of X_r with inlet **k** and e levels.

The inlet profile for e has to be assumed, since no measurements are possible. It **is** specified as

$$e = C_\mu k^{3/2}/(Const\ \ell) \qquad (2)$$

where ℓ is the length scale and $C_\mu = 0.09$ The variation of the constant from 1.0 to 0.003 does not change the predicted reattachment length appreciably Only when the constant is specified as 0.0003, i.e., $\ell = 0.0003H$, the reattachment length increases by about 0.8H. One point to note here **is** that the results show the correct expected trend. That is, with a larger inlet length scale (higher viscosity), the reattachment length is shorter For the case of the flow over a backward-facing step, such a trend was not observed [161

12

Moon and Rudinger [13] found experimentally that for Reynolds numbers greater than 10^5, the length of the recirculation was independent of the Reynolds number, Red (based on the upstream mean velocity and diameter). The predicted results show that the reattachment length increased slightly with increase in Reynolds number at low Reynolds numbers (Fig. 11), and for $Re_d > 10^5$, no significand change in X_r is observed as in the experimental results.
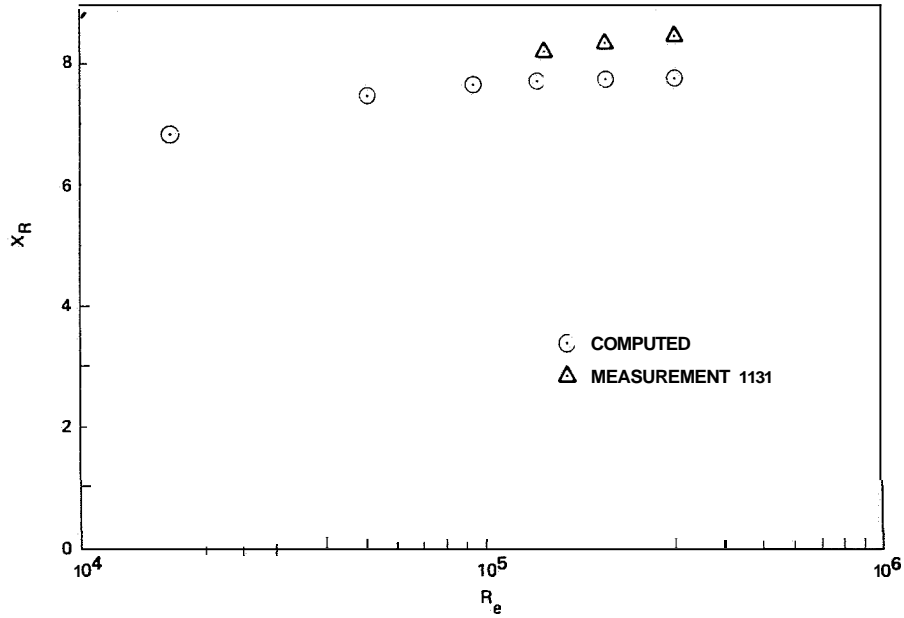
Figure 11. Variation of X_r with Reynolds number

The effect of expansion ratio D/d on the length of the separated region is shown in Figure **12** These results were obtained for a Reynolds number of 2.1 x 10^5 The recirculation length X_r **is** seen to increase with increase in expansion ratio for all the three cases. However, the variation is not linear **as** in the laminar flows. The difference in the values of X_r for axisymmetric expansion and plane
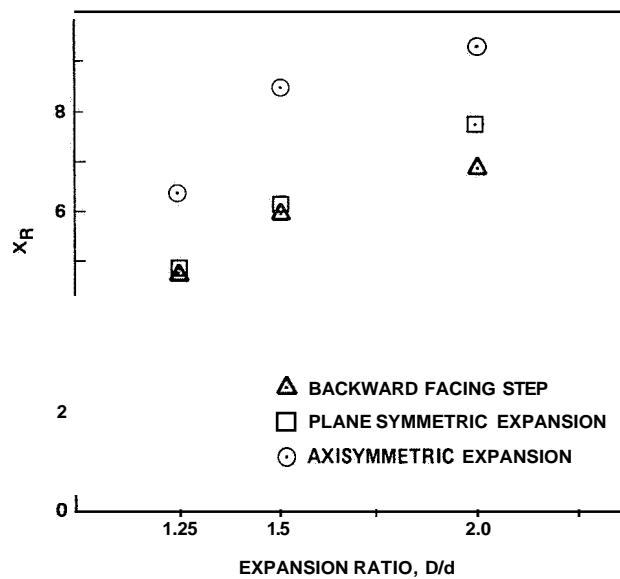
Figure 12. Variation of X_r with expansion ratio.

13

symmetric expansion is highest (2.3H) for an expansion ratio of 1.5   At the expansion ratio of 2, the plane symmetric expansion will be unstable and unequal regions of separation on either side of the centerline occurs. Here, the solution has been obtained by considering only one-half of the duct. As the expansion ratio becomes larger (=2), the stabilizing effect of the top wall becomes significant.

III. CONFINED FLOWS WITH/WITHOUT SWIRL

The study of axisymmetric confined flows actually involves three cases. (1) pipe expansion, (2) coaxial jet in confmed sudden expansion without swirl, and (3) coaxial jet in confined sudden expansion with swirl in the outer annular jet. The flow in a pipe expansion can be viewed as a coaxial jet having equal velocities between the annular jet and central jet, with the dividing lip of the central pipe being infinitely thin. Table 1 summarizes some of the important parameters of the cases studied. In these cases, the ratio of the velocity of the annular jet, U_a, to the velocity of the central jet velocity, U_p increases from 1 to 12. The difference between the central and annular jet velocities in a confined chamber will create different turbulence diffusion processes. The standard k-e model is used for the predictions of these flows with the same inlet flow turbulence level as calculated from equations (1) and (2). The sensitivity study of the initial boundary conditions on the flow fields for a specific case $(U_a/U_p = 3)$ will be presented in Section III.B.

TABLE 1   CONFINED COAXIAL JET WITH DIFFERENT U_a/U_p

| Case	Reynolds Number	U_a/U_p	D_a/D_p	D_o/D_a	Exp. X_r/H	Predicted X_r/H
Moon and Rudinger [13]	2.611×10^5	1		1.43	8.7	7.2
Habib and Whitelaw [19]	$Re_p = 39900$ $Re_a = 55200$	1			9.25	8.2
	$Re_p = 20600$ $Re_a = 85000$	3	2.76	2.81	10.25	8.4
Johnson and Bennett [20]	$Re_p = 15900$ $Re_a = 47500$	3.1 1	1.93	2.07	7.2	8.1
Owen [21]	$Re_p = 8000$	12	1.4	1.43	3.73	4.0

A, Pipe Expansion/Coaxial Jet: No Swirl

The effects of various central jet/annular jet velocity ratios on the flow field can be reflected by the computed corner recirculation zone length X_r which are listed in Table 1   The reattachment length for the coaxial jet with $U_a/U_p = 1$ is also shown. The wake created by the finite thickness **of** the pipe wall in coaxial jet flow extended to about one and a half chamber diameter downstream [Fig. 14(b)] , which produced extra longitudinal strain   This can influence the length of the recirculation zone. **As** it can be seen from Table 1, an increase in the velocity ratio (U_a/U_p) from 1 to 3 leads to a larger region of recirculation zone. Habib and Whitelaw [19] reported 10 percent increase in the length of the recirculation zone for the higher velocity ratio $(U_a/U_p = 3)$ in their measurements. The k-e model prediction
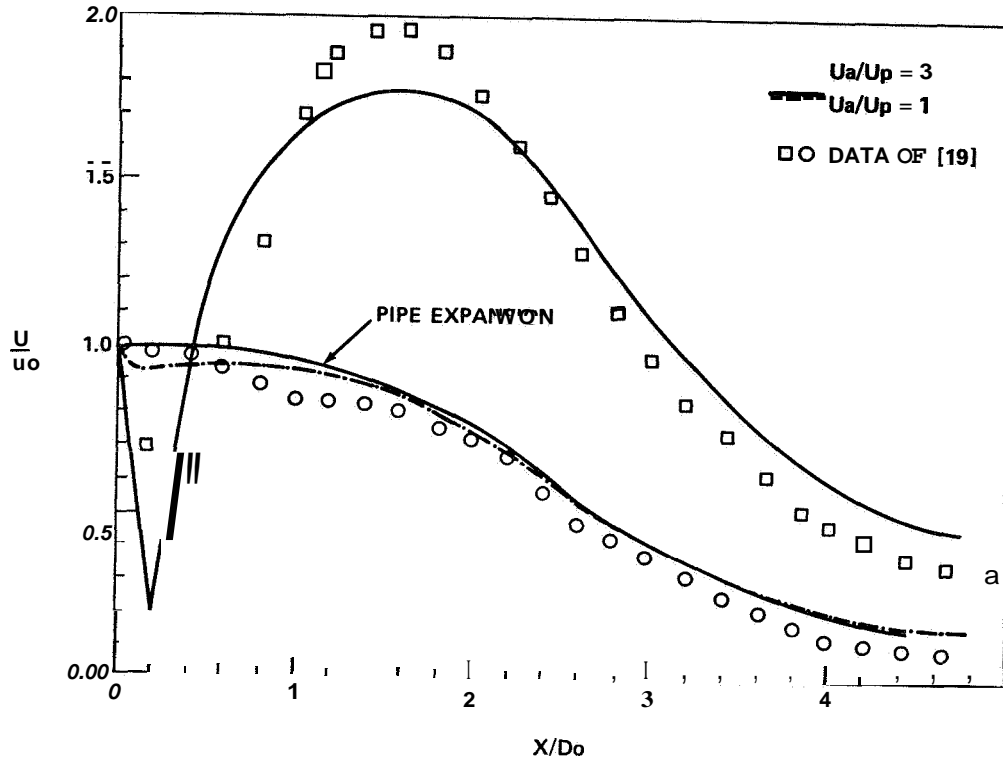
14

Figure 13   Variation of centerline velocities.

underestimates this increase (about 2 percent increase). For a similar experimental study by Johnson and Bennett [20] the calculated X_r has a similar magnitude as the one calculated from Habib and Whitelaw's case, However, the measured X_r of the latter is longer than the former. This may be attributed to the Reynolds number dependence as discussed in Section II.B. For the case of $U_a/U_p = 12$, because of the large momentum difference, a large central recirculation zone was formed just downstream of the expansion. The strong shears created by the high velocity ratio of the annular and central jets largely enhance radial mixing thus reducing the region of the corner recirculation zone. This phenomenon is similar to that observed in the confined coaxial jet with strong swirl in the annular region (Section III.C).

In Figure 13, the calculated centerline velocities for the confined coaxial jet with different ratios of the annular jet velocity to the central jet velocity are shown. The higher velocity ratio jets show more rapid mixing and decay compared to those for $U_a/U_p = 1$ in the axial direction. Also shown in Figure 13 is the decay of centerline velocity of the pipe expansion flow In the region just downstream of the expansion, the decay of the coaxial jet with $U_a/U_p = 1$ is substantially faster than that of pipe expansion flow The experimental data of Reference 19 are also shown. The predictions are in fairly good agreement with the measurements. As suggested by Keference 19, the overprediction of mean velocity for unity velocity ratio and underprediction for a velocity ratio of three probably stem from the incorrect representation of the turbulent-diffusion process in the k-ϵ model. Other possible discrepancies may be caused by the specification of the inlet values of k and ϵ which have appreciable influence on the turbulent-diffusion process in the region downstream of the expansion. Figure 14 shows the normalized mean axial velocity profiles as a function of the radial location at different axial stations, X/D_0, along the confined chamber for cases $U_a/U_P = 1$ and $U_a/U_P = 3$. At the plane just downstream of the expansion

15
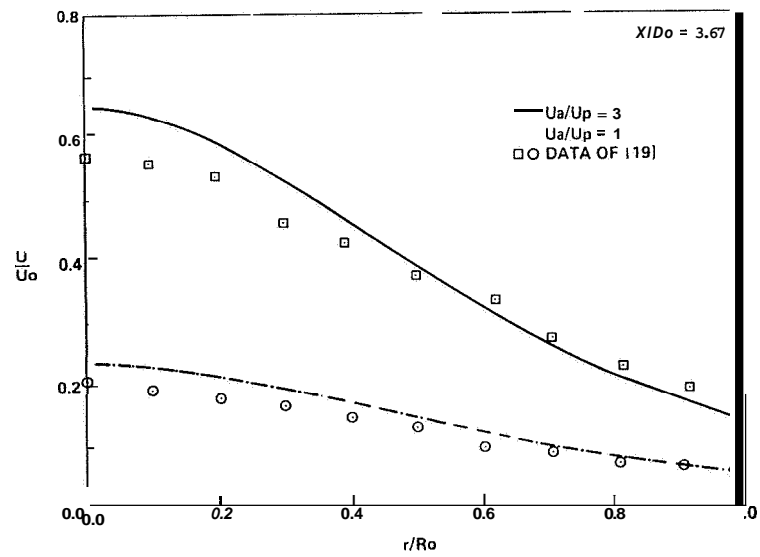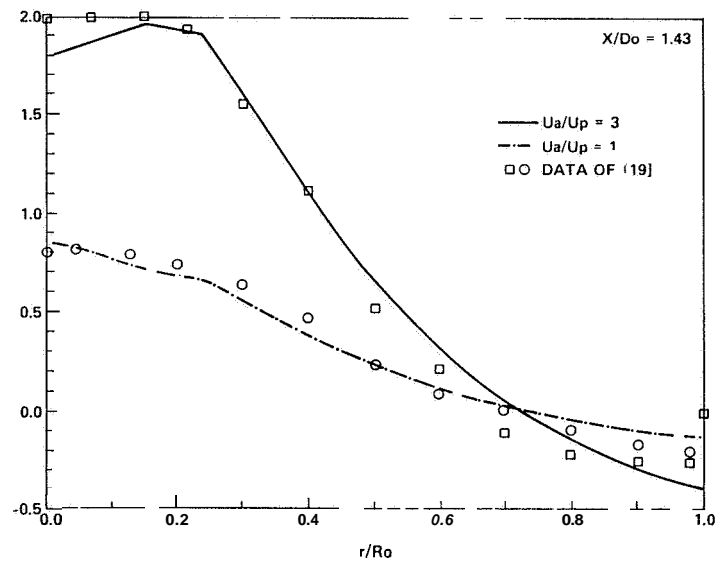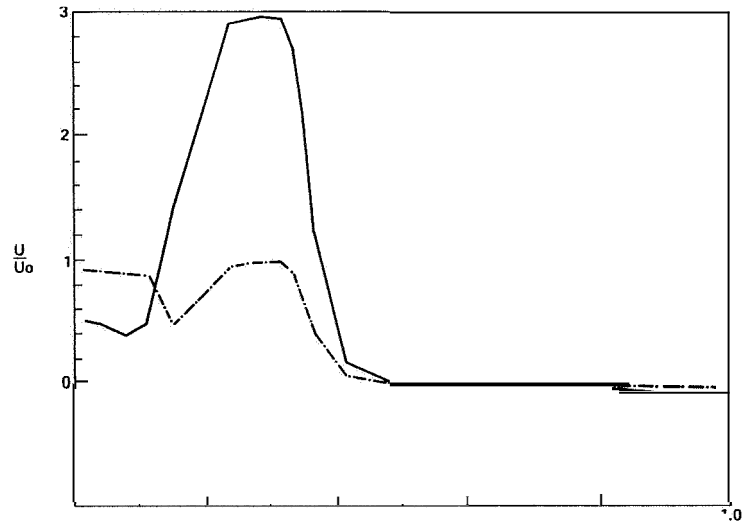
Figure 14. Mean velocity profiles, X/D_O = 0.1, 1.43, 3.67
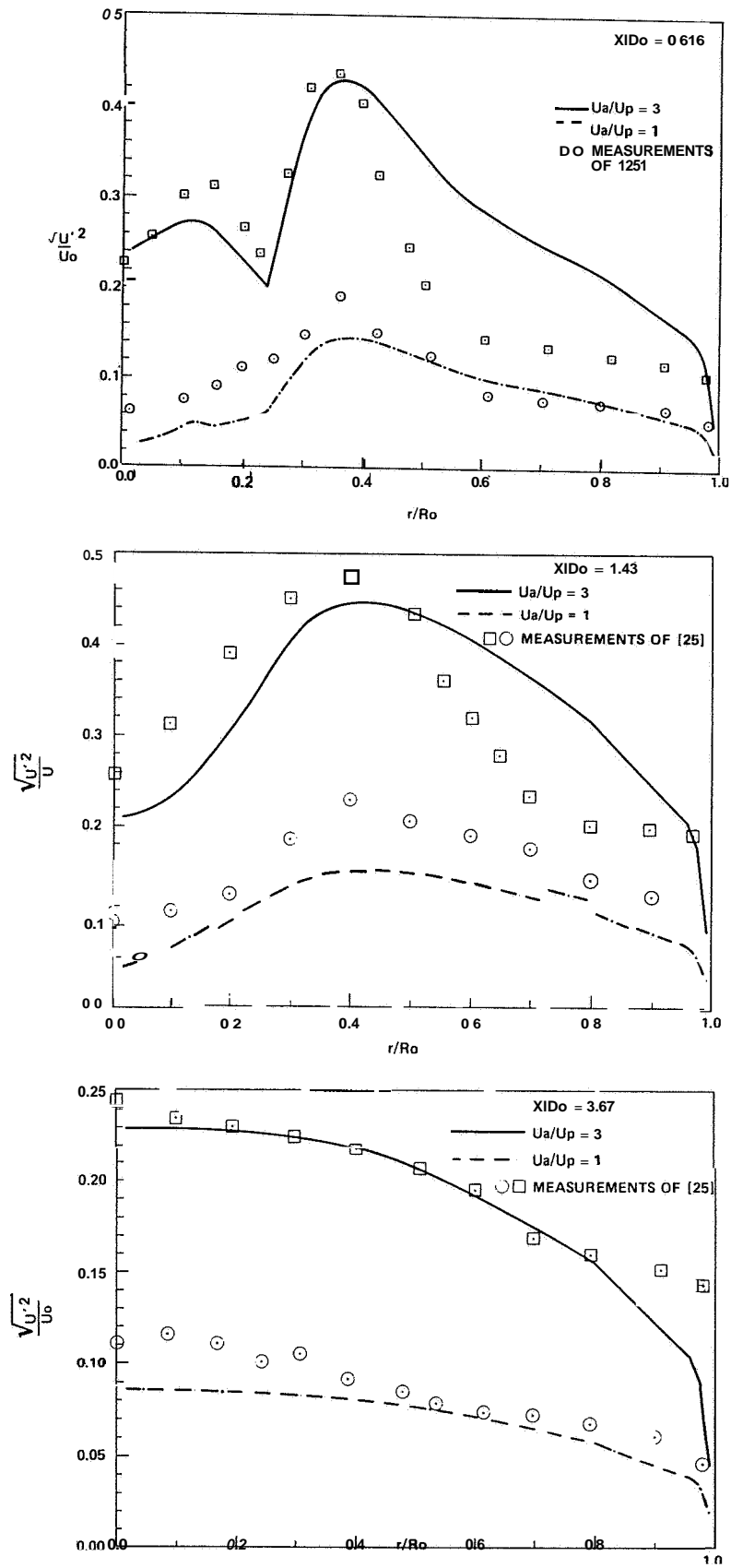
Figure 15. Radial profiles of axial fluctuations at X/D_o = 0.6 16, 1.43, 3.67

($X/D_o = 0.1$), the faster decay of the central jet for the velocity ratio $U_a/U_p = 3$ is clearly caused by the strong shear created by the velocity difference between U_p and U_a The minimum velocities in the wake region are due to the finite thickness of the inner pipe wall. The extent of the wake region is shorter for the case of higher velocity ratio ($U_a/U_p = 3$) because of the rapid mixing in the radial direction. The predicted radial distributions of mean velocity compare fairly well with the measurements in the downstream region. However, the inaccurate velocity peak predicted at $X/D_0 = 1 43$ indicates the deficiency of isotropic eddy viscosity hypothesis used in the **k-e** model.

The longitudinal turbulence intensities normalized with U_p are shown in Figure 15. The predicted fluctuating quantities are derived from the isotropic turbulence assumption of k-ϵ model, thus

$$(\overline{u'^2})^{1/2} = \left(\frac{2k}{3}\right)^{1/2}$$
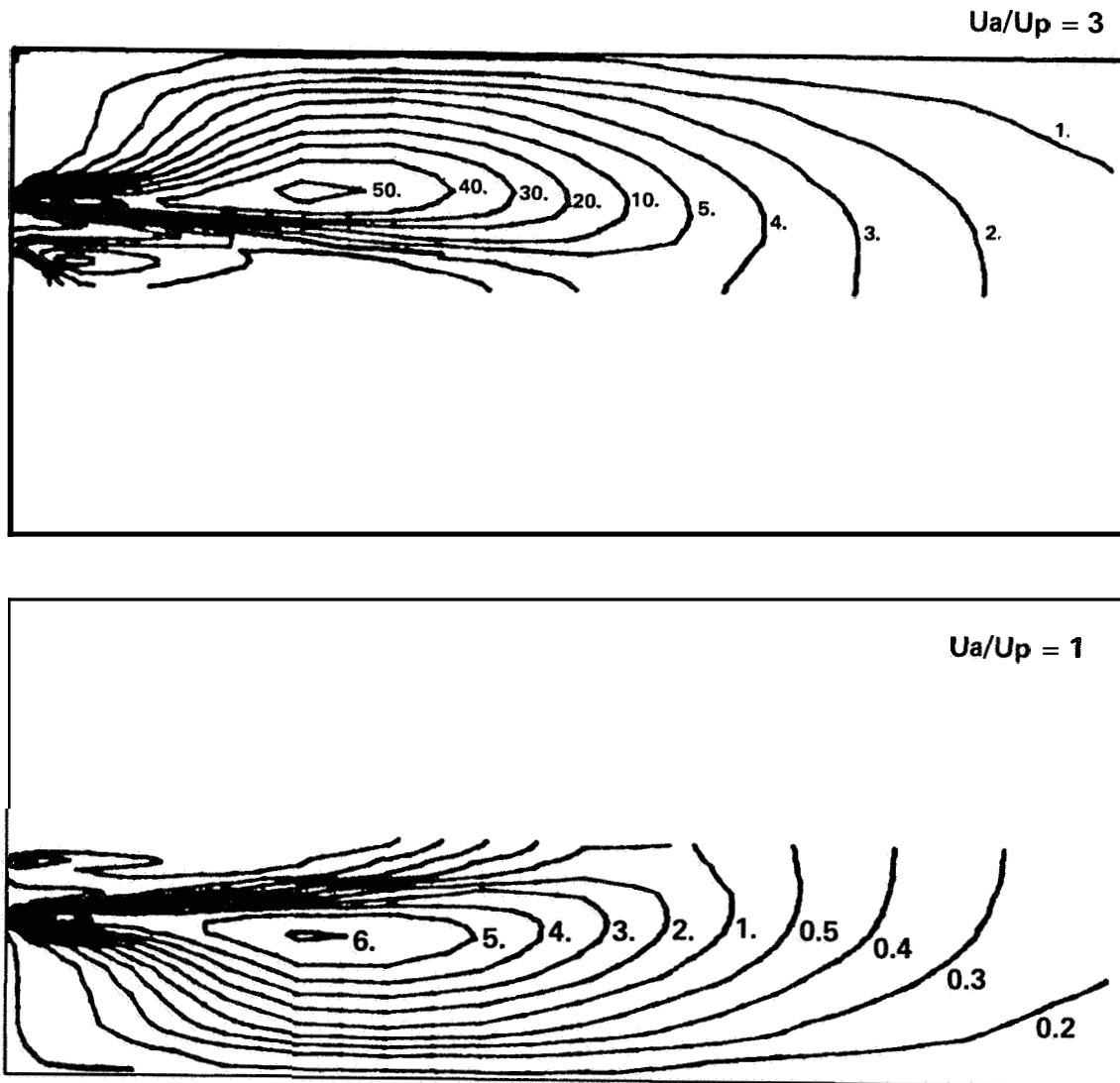
Figure 16. Contours of kinetic energy.

Just downstream of the expansion, the maximum fluctuation occurs in the separated region. However, further downstream of the expansion, even after the reattachment point, the maximum fluctuation does not move close to the wall as would be expected. The pattern of the results can be further observed from the kinetic energy contours shown in Figure 16. These results show a distinct difference compared to the axi-symmetric pipe expansion flow (Figs. 6 and **7**). The difference **is** likely attributed to the differences in the grometies, and that the confined coaxial jet has not reached the fully developed pipe flow at the exit plane of the calculation domain. The predicted axial fluctuations show correct qualitative trend for the confined coaxial jet without swirl, observed in experiments. The discrepancies in the upstream region predictions could well be due to the inadequate specification of inlet boundary conditions at the exit of central and annular jets. The sensitivities of the inlet boundary conditions on the development of the non-swirling coaxial jet will be addressed in the next section,

B. Sensitivity to Inlet Boundary Conditions of Non-Swirling Flows

In this section, the influences of inlet plane boundary conditions on calculated values of dependent variables are presented. The test case chosen is the confined coaxial jet with a sudden expansion with $U_a/U_p = 3$ of Habib and Whitelaw [191 In addition to the assumed shape of the radial profiles of the mean axial velocity, different levels of turbulence quantities such as k and e which are normally not known at the expansion plane will be tested to indicate the sensitivity of the inlet boundary conditions.

The first case tested was the influence of the assumed shape of the velocity profile at the expansion plane. The entry profiles of k and E were calculated from equations (1) and (2). The calculations show that the specification of uniform velocities at the annular and central Jets lead to downstream values of the centerline velocity which are about 1 percent higher than those obtained with a 1/7-law velocity profile The calculations also show an insignificant increase in X_r (~1 percent) for the fully-developed initial-velocity profiles as compared to the uniform-velocity profiles, The influence of the initial-velocity profiles can therefore be neglected.

In the following calculations, the mean-axial velocities are assumed uniform across the inlet plane. Usually, distributions of turbulence quantities such as k and e are not available from the experiments at the inlet plane, but are necessary for the calculation scheme as inlet conditions. Different initial turulent kinetic energy and energy dissipation rate would affect the eddy viscosity, 1.e. the momentum transfer process. This may sometimes change the flow characteristics further downstream. Figure 17 presents results using three distributions of turbulent kinetic energy corresponding to (1) a uniform distribution with $k/U_{in}^2 = 0.003$, (2) a distribution with 0.003 at the central nodes and 0.009 at the three near wall nodes, this profile was used to simulate a kinetic energy distribution in a fully developed pipe flow, and (3) a profile taken from Reference 31 with an empirical formulation for the fully developed pipe and annular flows

$$
k = \begin{cases}
(0.035\ U_{in})^2 \left[2 + 8\left(\dfrac{r}{R_i}\right)^2 \right] & , 0 \leqslant r \leqslant R_i \\[4em]
(0.035\ U_{in})^2 \left[2 + 4\left(\dfrac{r}{R_s}\right)^2 + 4\left(\dfrac{r}{R_o}\right)^2 \right] & , R_s \leqslant r \leqslant R_o
\end{cases}
\tag{3}
$$
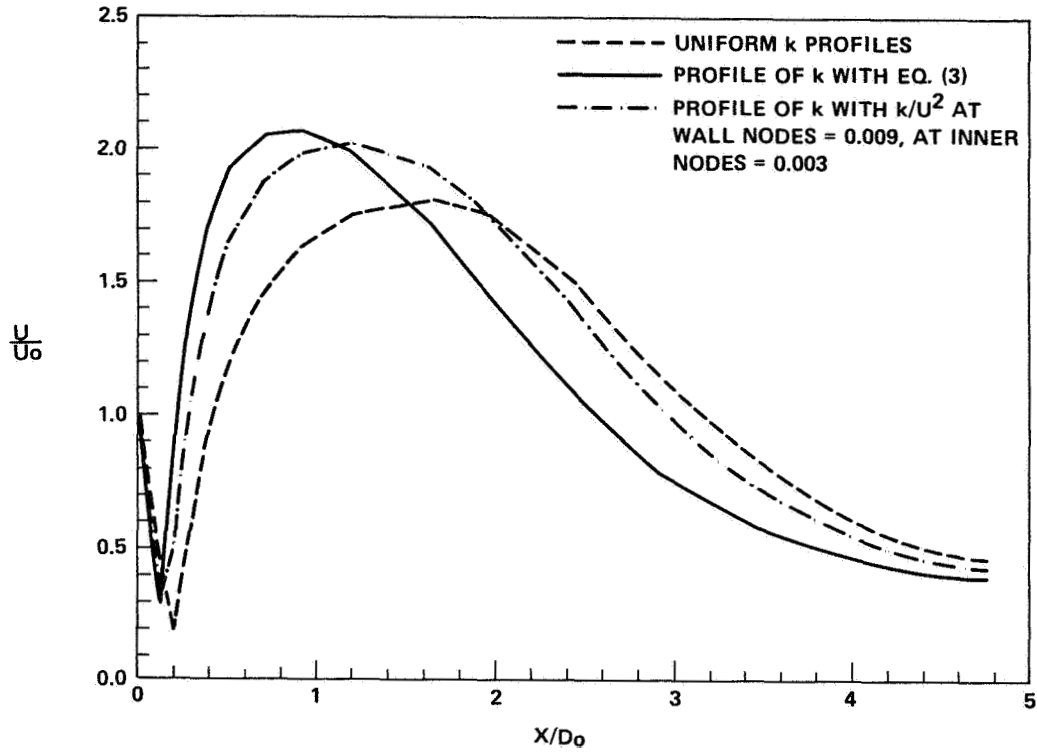
Figure 17 Influence of initial profiles of kinetic energy on mean velocity

The corresponding values of dissipation rate were determined from equation (2). The results show that the influence of the inlet profiles of kinetic energy is significant The influence upon the center-line mean velocity of an increase in the normalized kinetic energy from 0.003 to 0.009 at the three near-wall grid nodes is to shift the minimum velocity toward the flow entrance because of the large eddy viscosity assigned near the wall region, which enhances the spreading and decay of the central jet in the initial region The difference is also reflected in the regions away from the centerline and the entrance plane. The predicted recirculation zone length is appreciably shorter (10 percent) and the negative velocities attain lower values (≈ 7 percent) for the case of "clipped" kinetic energy profiles. The underpredictions of the maximum velocities after $1\ D_o$ mentioned in Section III.A is much improved as a result of the new boundary conditions in k However, the inlet level of turbulence has significant influence on the kinetic energy distribution along the chamber Too much turbulence is introduced as a result of too large a kinetic energy in the initial region (Fig. 18)

Finally, the importance of inlet ϵ is considered here Estimation of e at the inlet plane usually is achieved by the mixing-length formulation [equation (2)] Another procedure of extracting e found in the literature was based on the isotropic eddy viscosity formulation

$$\epsilon = -C_\mu \frac{k^2}{\rho\ \overline{u'v'}} \frac{\partial U}{\partial r}$$

20
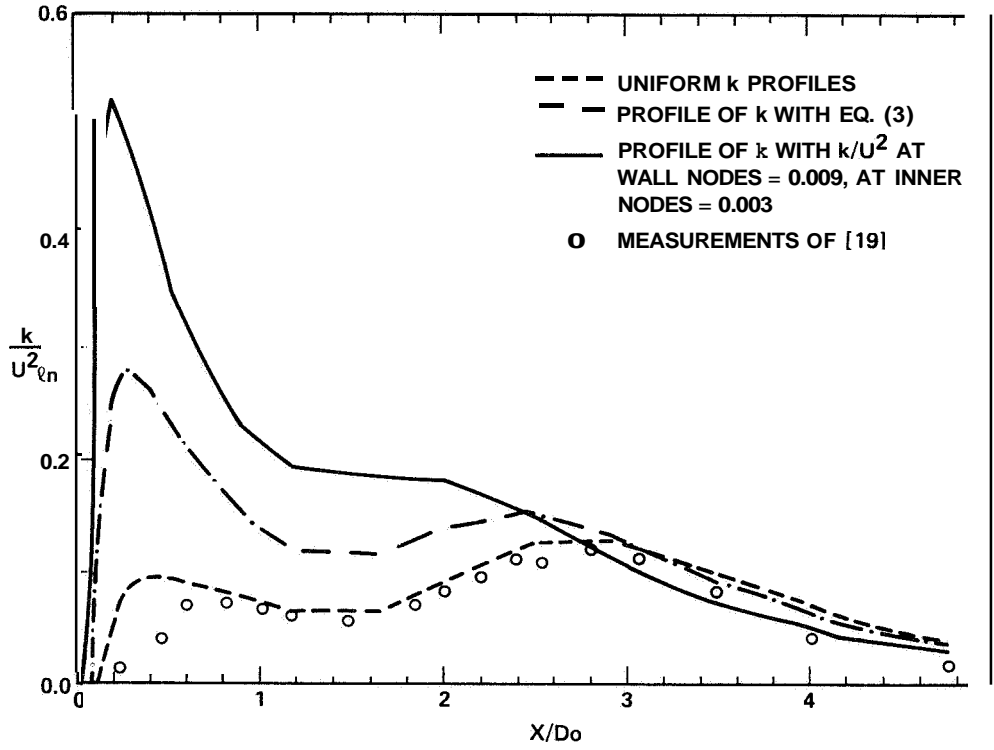
Figure 18. Influence of initial profiles of k on centerline turbulent kinetic energy

if u'v' and k were measured at the inlet plane, Equation (2) requires the specification of a characteristic dimension related to turbulent eddy size, ℓ' The inlet distribution of length scale has a large effect on the flow field in the upstream region where the diffusion term is important, The test of the inlet e level was performed by varying the e within the range $0.5\,\epsilon_r \leqslant \epsilon_r \leqslant 2\epsilon_r$, where ϵ_r is the reference level of the E calculated from equation (2). **As** seen from Figure 19, the level of the e has appreciable influence on the calculations. **As** a matter of fact, the specification of appropriate initial turbulence level (**k** and ϵ) plays a role of equal important to turbulence-model corrections as will be seen in Section III.C Further testing on the ϵ level was carried out assignmg the different distribution of ℓ' across the inlet plane The first case was to change the value of ℓ' in the annular exit using R_0 instead of the annular width (R_0-R_s) [22] The second case mvolved using **an** empirical correlation of the length scale distribution across the pipe and annular region, the expression of ℓ' is given by [23]

$$\ell' = \begin{cases} R_i \left[0\,14 - 0.08 \left(\dfrac{r}{R_i}\right)^2 - 0.06 \left(\dfrac{r}{R_0}\right)^4 \right] & 0 \leqslant r \leqslant R_i \\[4mm] 0.014\,R_0 \left[\left\{ \left(\dfrac{R_0}{R_s}\right)^2 + 1 \right\} \left(\dfrac{r}{R_0}\right)^2 - 1 - \left(\dfrac{r^2}{R_s R_0}\right)^2 \right] & R_s \leqslant r \leqslant R_0 \end{cases} \tag{5}$$

The effects are shown in Figure 20 on the centerline-velocity decay and in Figure 21 on the e profile along the chamber The different specification of length scale distribution has a large effect in

21
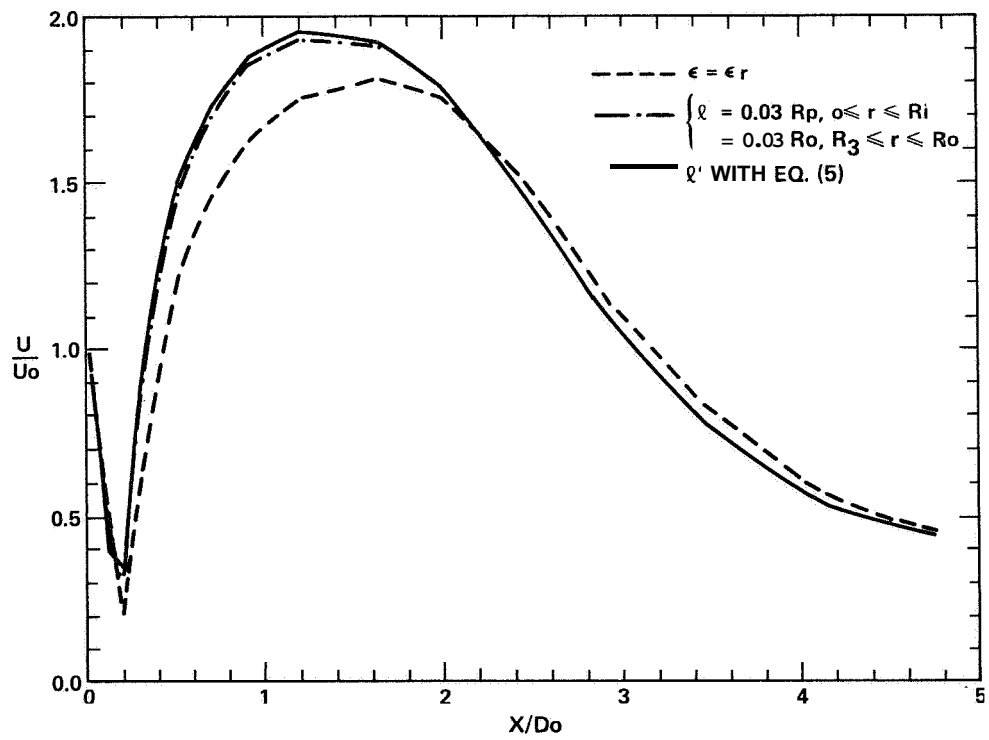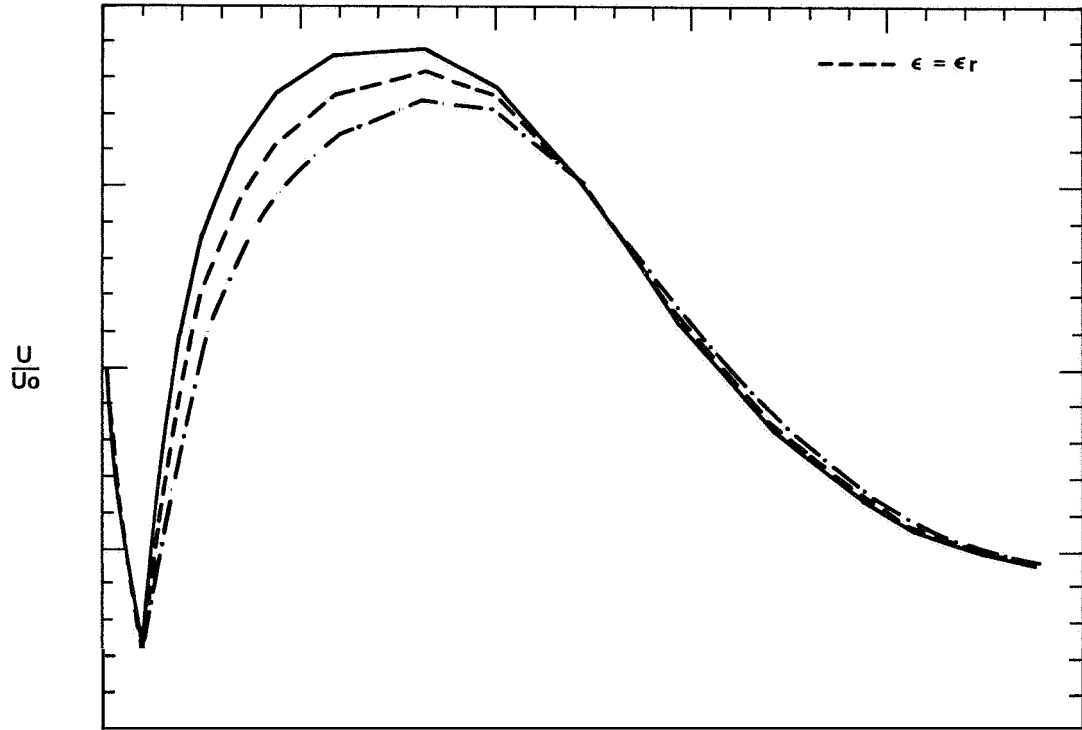
Figure 20, Influence of initial profiles of E on mean velocity
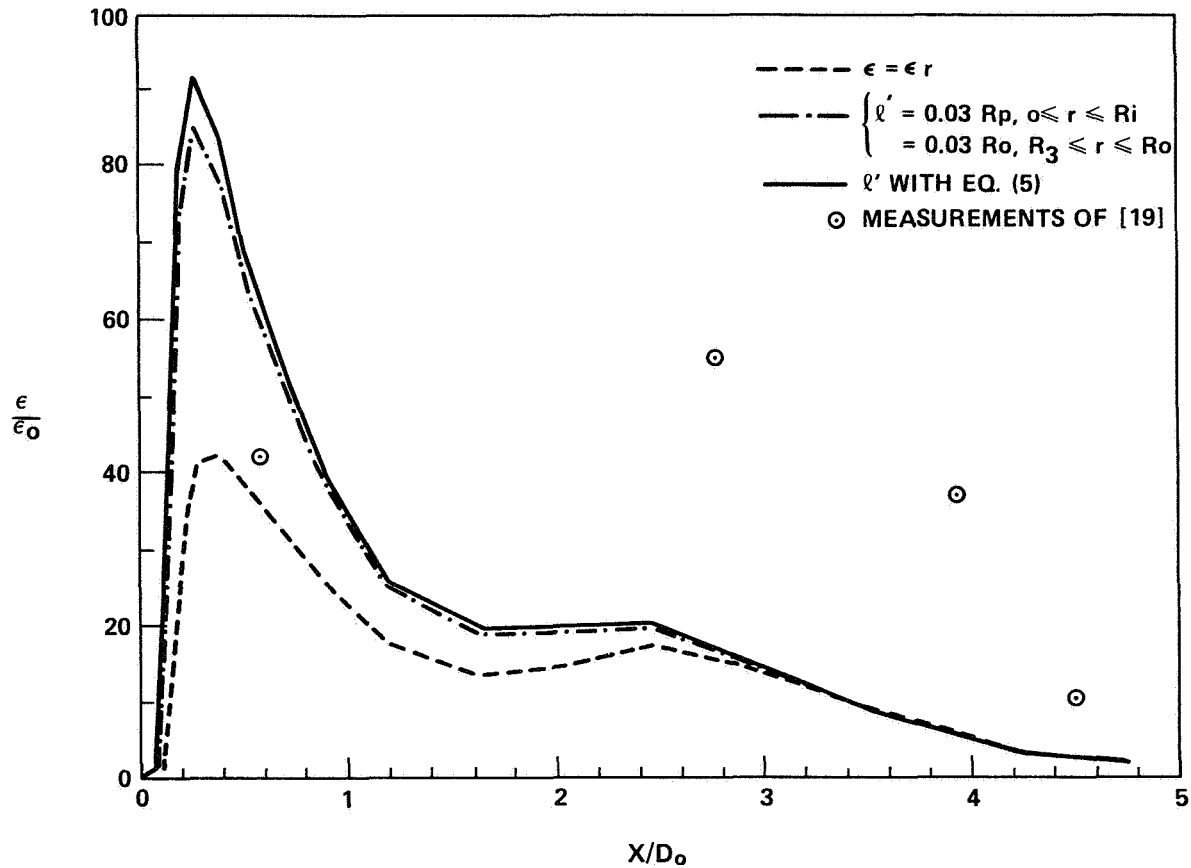
Figure 21 Influence of initial profiles of ε on the rate of dissipation

the upstream region where the diffusion terms have a large effect on the mean velocity, it has no significant effect in the downstream region where the diffusion effects are minimal. If the swirl is introduced to the flow field, the turbulent diffusion process will be compounded by additional streamline curvature and extra strains, the calculations of the confined swirling flows are described in the next section

C. Confined Swirling Flows and the Sensitivity to the Inlet Boundary Conditions

The introduction of swirl into the flow creates much faster mixing, caused by radial pressure gradients and increase in the turbulence generation   The flow field in a confined swirling jet is more difficult to predict due to the streamline curvature effect produced by the swirl and the strong anisotropy of the turbulence.   In the study of confined coaxial swirling jets, the swirl is introduced through the annular flow   This study is essentially an extension of the confined coaxial jet and the geometrical configurations are the same as the ones used in Section III.A   The azimuthal velocity profile of the annular flow can be a solid body rotation, a free vortex structure or just simply flat swirl velocity profile depending on the design of the swirl vanes used at the entrance of the expansion   The overall swirl strength at the inlet plane of the expansion chamber is usually characterized by the swirl number **S,** which is a non-dimensional number representing axial flux of swirl momentum divided by axial flux of axial momentum, times the equivalent nozzle radius.   In a coaxial swirling jet, S can be written as

$$S = \dfrac{\displaystyle\int^{R} r^2\, UW dr}{R_O \displaystyle\int^{R} r \left(U^2 - \dfrac{W^2}{2} \right)}$$

When swirl is introduced in the annular flow in the confined coaxial jet, significant radial and axial pressure gradients are set up near the central jet exit. At high degrees of swirl ($S \geqslant 0.4$ in confined coaxial jet), these pressure gradients would result in axial recirculation in the form of a central toroidal recirculation zone which is characterized by the presence of low tangential velocities, high turbulent intensities and large energy dissipation rates. The forming of the central toroidal recirculation zone depends on many factors, in addition to the swirl number, for example, size of enclosure chamber, geometry of the enclosure chamber, design of swirl vanes, and the inlet plane boundary conditions suck as particular velocity profiles and turbulence intensities. The more detailed descriptions of the current research activities in swirl flows can be found in Reference 24.

Computations for the confined coaxial jet with swirl were initially made with two configurations, (i) Habib and Whitelaw [25] and (ii) Roback and Johnson [26]. These two configurations were basically extensions of the non-swirling jet cases of Habib and Whitelaw [19] and Johnson and Bennett [20] (Table 1). In Habib and Whitelaw's case, tangential entrance was used to generate a forced-vortex-type tangential velocity profile with $S \cong 0.23$. For the case of Roback and Johnson, a free-vortex type tangential velocity was generated by swirl vanes at the upstream of the expansion plane with $S = 0.46$. Because of the different swirl generator and the different swirl strength involved, the development of the two flow field shows drastic differences. Shown in Figure 22 is a comparison of the calculated mean axial velocities along the centerline with the experimental data. For the case of $S \cong 0.46$ a central
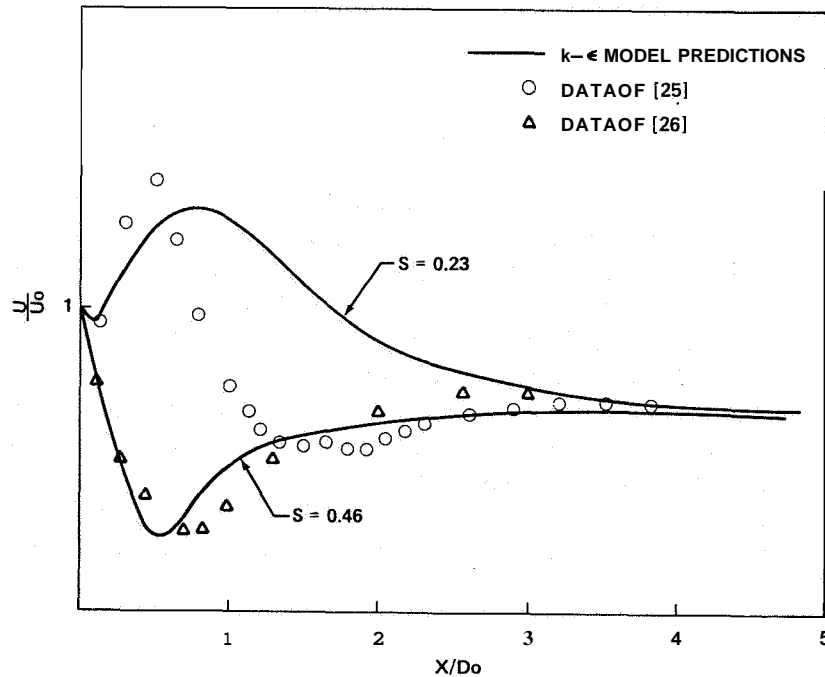

Figure 22. Variation of centerline velocity $S = 0.23$ and $S = \textbf{0.46.}$

24

recirculation zone appears in the initial region of the central jet. The present calculations with the grid 23 x 24, which is close to the grid used by a similar study [14], show very poor agreement with the measured data for the case $S \cong 0.23$. Further refinement in the grid system does not show any improvement. Some difficulties were encountered in a similar study by Sturgess [27] In his study, Sturgess indicated that fair comparisons could be obtained by careful placing of the gridlines, and the poor performance of the calculations resulted from the shortcomings of the physical turbulence model. Habib and Whitelaw [25] pointed out that the intermediate swirl number of 0.23 provides a flow which is probably more difficult to predict in that the near recirculating region is located away from solid surface and expansion plane. Different inlet conditions have been used as described in Section III.B trying to improve the calculations of centerline velocity distributions. With the higher level of kinetic energy prescribed for the inlet stream, which is shown to be very effective for the non-swirling case (Fig. 17), only in the very upstream region $X/D_O \leqslant 0.5$ the improvement is seen (about **5** percent); it has no significant effect in the downstream region ($\sim X/D_O > 1$) The serious discrepancies of the calculations for the intermediate swirl number case stem from the defects of the k-ϵ model which is incapable of taking anisotropic and streamline curvature effects in the predictions.

With a high swirl number, the recirculation region is closely tied to the expansion geometry and the downstream flow is more easily presented by the calculation methods. The subsequent calculations of the swirling confined coaxial jet with associated inlet boundary condition sensitivity test thus are presented for the high swirl number case ($S \leq 0.46$). Figure 23a shows the results using the distributions of kinetic energy corresponding to equation (1) and equation (3). The influence of the inlet stream turbulence on the centerline velocity distribution is not as significant as the non-swirling case (Fig. 17). The diffusion process induced by the strong swirl is more important than that involved by the inlet turbulence level. Thus the specification of the inlet tangential velocity profile is extremely important for the calculations of swirling flows. In fact, Ramos [5] showed that by using a Rankin-vortex type tangential velocity profile at the inlet plane of a swirling coaxial jet without expansion, k-ϵ model gave drastically different predictions compared to the forced-vortex type tangential velocity specification at the inlet plane for both co- and counter-swirl flow conditions. A similar trend is found for the different specification of initial dissipation rate. In Figure 23b, the calculations were made with the inlet distributions of length scales estimated from equation (2) and equation (5) Also shown in Figure 23 are the predictions made with the modified k-ϵ model based on the flux Richardson number correction of the ϵ-equation [28] The effect of inlet e level is appreciable only in the initial region In a free-swirling jet study of Leschziner and Rodi [6], the influence of the initial turbulence level was found to extend to the far downstream. In the confined-swirling flow, this influence is not significant in the downstream region In the upstream region, however, the specification of appropriate initial turbulence level (**k** and E) plays a role at least as important to turbulence-model corrections as seen in Figure 23,

IV. COMPARISON OF THE PREDICTION OF PHOENICS AND TEACH CODES

PHOENICS and TEACH codes use the same form of the time averaged equations governing the flow and the k-e turbulence model in which the differential equations for turbulence kinetic energy, k, and its dissipation rate, *e*, are employed. These equations are expressed in a general form and the appropriate source term for each dependent variable is added [10] The equations are solved using finite difference techniques.

Both the codes employ finite volume method of discretization in which integration is carried out over an elementary domain bounded by distinct lines of network. PHOENICS code used in the present computations employs an upwind difference scheme while TEACH employs a hybrid, central-upwind
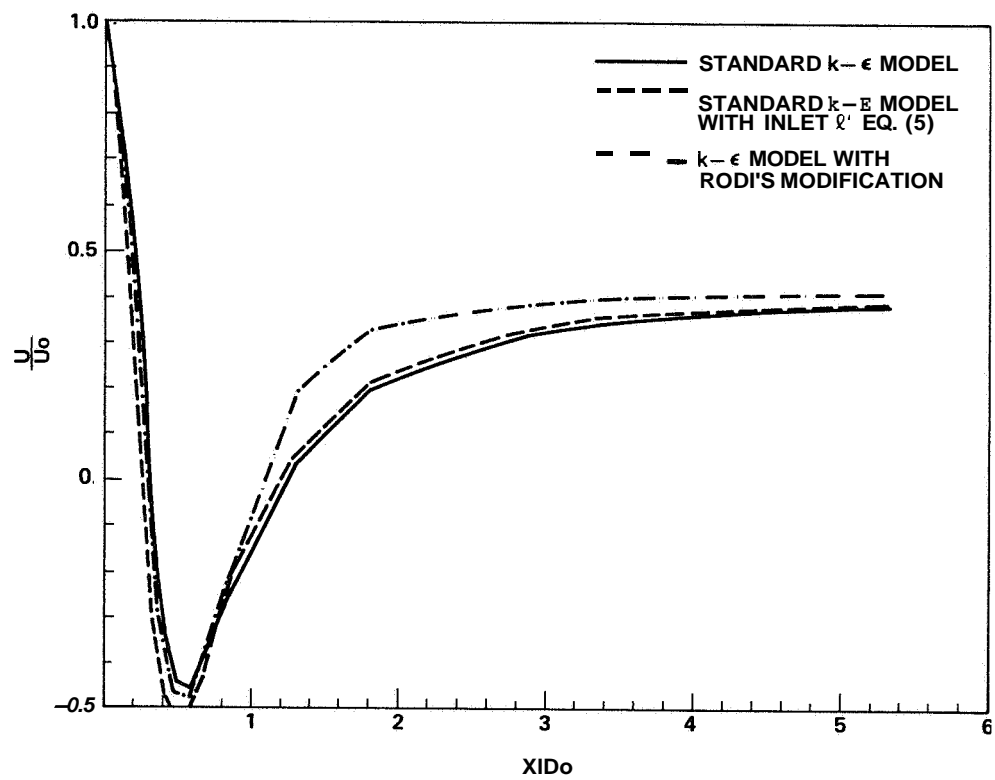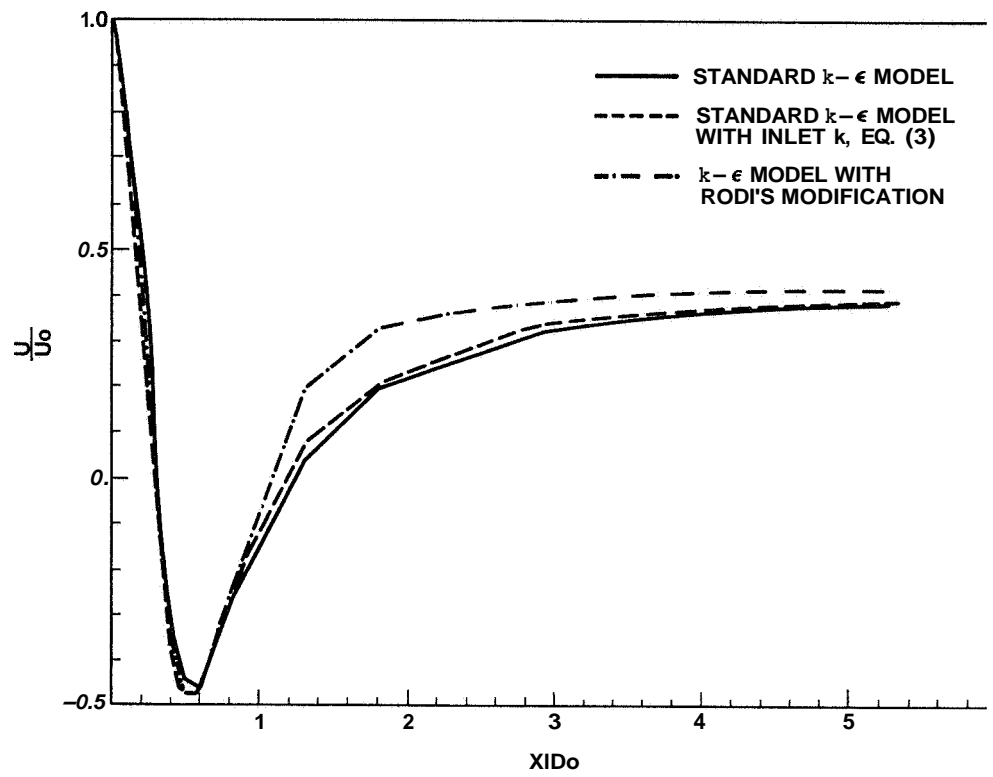
Figure **23.** Influence of initial profiles of **k** and E on mean velocity swirling flow

scheme. Near wall treatment is through the wall function method. However, details of the design and execution of the solution algorithm may differ   One wishes that the codes would predict correctly the physical problem at least qualitatively and would produce quantitative results as close to the measurements as possible.

During the present investigation some discrepancies between predictions of the two codes have come to light. These are briefly described here to let the users of these codes know the deficiencies. Efforts should be made to improve the algorithms. The predictions compared here are for the flow in a sudden pipe expansion with an expansion ratio of **2.**

In a sudden pipe expansion, high shearing rates are generated in the separated layer (away from the wall). In this region turbulence energy generation rate will be large due to the high shear, while dissipation rates will be low because they are away from the wall. The turbulence energy level thus increases rapidly to magnitudes many times larger than the regular pipe flow. The magnitude of the energy reduces further downstream and beyond reattachment point the flow develops to regular pipe flow. Thus, as discussed in Section 11, just downstream of the expansion, the kinetic energy maximum should occur in the separated layer, further downstream the maximum moves close to the wall. After the reattachments, the flow redevelops and attains the full developed profile.

The kinetic energy contours predicted by the two codes are shown in Figure 24a. It is seen that the PHOENICS prediction produces kinetic energy contours in qualitative agreement with measurements, while the prediction of TEACH produces qualitatively different distribution of kinetic energy in some regions of the flow   The reason for this is not known   However, such contours have also been reported in the literature (see for example, Gosman, et al. [29] (Fig. 10a). TEACH prediction shows that the k-maximum moves quickly toward the centerline of the pipe. Detailed examination of the algorithm is essential to explain this behavior of **k** and to incorporate modifications to rectify this problem.

Another comparison is that of the important quantity, the size of the recirculation region. Both the codes predict the length of the reattachment more or less closely   However, the locus of flow reversal (U = 0 contour) line is not predicted well. In addition, the PHOENICS code produces a long tail for the recirculation region. Physically such a long thin recirculation region cannot exist. If the tail is ignored the predicted length X_r will be significantly smaller than the experimental value. Since PHOENICS code uses an upwind scheme, the false diffusion can influence the size of the recirculation region, It is not clear whether that is the reason for the observed results. The long tail region is also exhibited in the PHOENICS Demonstration Report by Qin [15]

The implementation of the wall functions seems to be different in both the codes. As discussed in Section 2, the nodal point adjacent to the wall has the highest return flow velocity and at the next point the velocity drops down sharply   This occurs in both codes. However, TEACH produces a smoothed velocity profile while PHOENICS produces a highly peaked profile as shown in Figure 24b.

In TEACH code, special efforts are required to include blockages/irregular geometry etc. Hence, most of the computations of expansion flows, coaxial jets etc. using TEACH code, start the computation at the expansion plane. Thus, the important upstream effects on the flow as it arrives at the expansion are lost. Specifically, the kinetic energy profile at the expansion plane in both cases would be distinctly different. This has significant influence on the flow downstream. For example, the predicted reattachment length can differ by as much as one step height, i.e., is more than 10 percent, in the pipe expansion flow   As would be expected, the computations start upstream and predict a larger X_r. The X_r, thus predicted agrees more closely with the experimental measurements, since experimenters usually provide "enough" starting length.

PHOENICS

TEACH

(a) k contours.

X/H = 4

- - - - PHOENICS
_____ TEACH

U (m/sec)

r/R
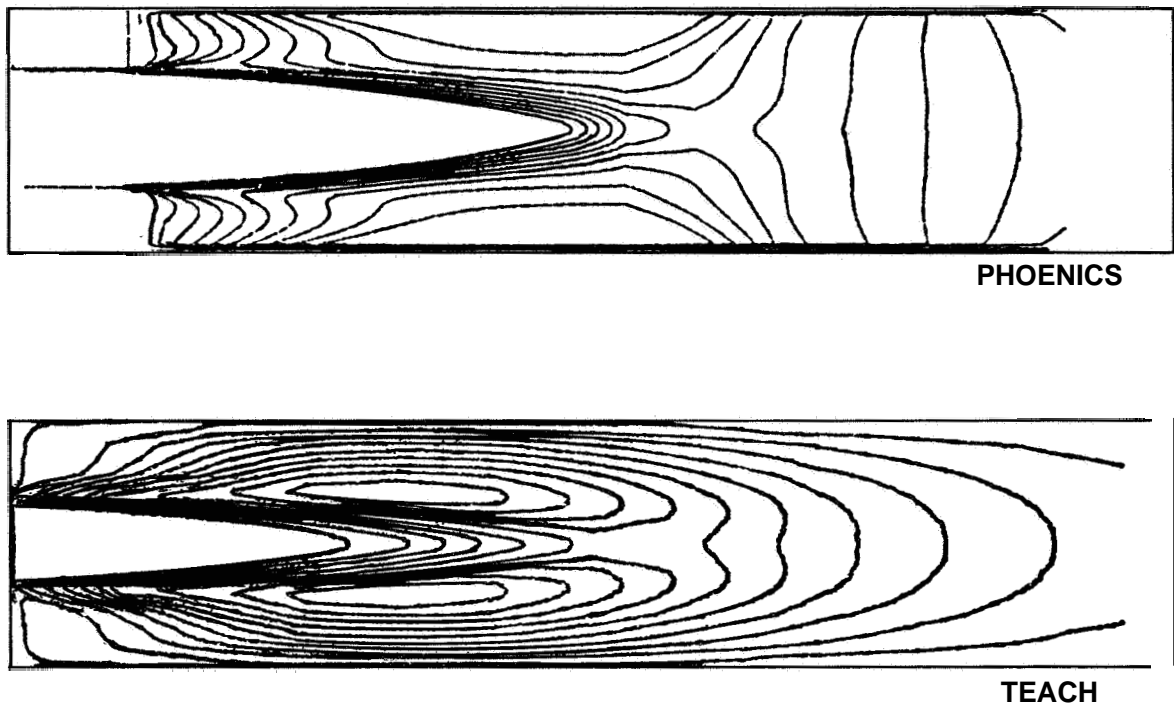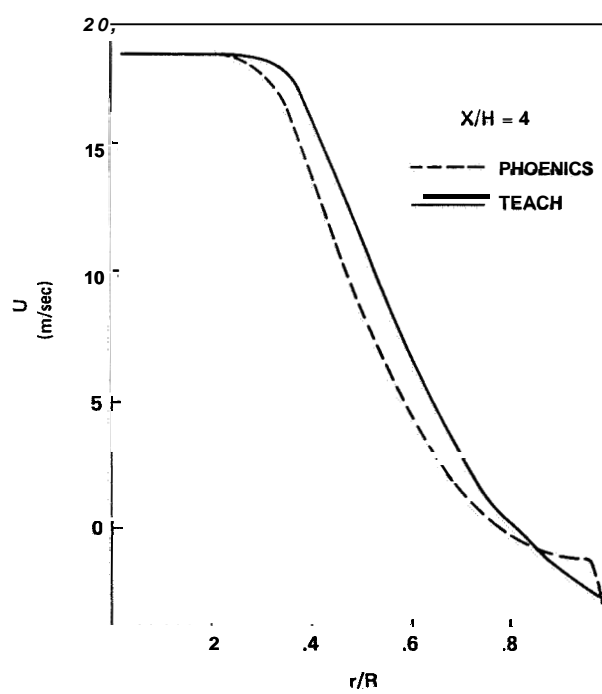
(b) Flow reversal and velocity profile.

Figure 24   Comparison of PHOENICS code and TEACH code,

Thus, it is observed that the widely used PHOENICS and TEACH codes require some modifications to produce predictions which would agree more closely with the experimental observations.

V. CONCLUSIONS

1) The severe underprediction of the length of the separated region in the case of the flow over a backward-facing step is related to the stronger streamline curvature in the initial region of the separated layer as compared to the axisymmetric flow

2) In the case of the flow in a sudden pipe expansion, a larger inlet length scale produces a shorter reattachment length, as expected.

3) The predicted reattachment length becomes independent of Re only for $Re > 10^5$

4) At higher expansion ratios, the stabilizing effect of the wall in the symmetric expansion is significant.

5) The finite thickness of the dividing lip at the expansion plane of the confined coaxial flows has significant influence on the flow development   The large difference of the corner recirculation zone length between the coaxial jets with high velocity ratio ($U_a/U_p = 3$) and unity velocity ratio ($U_a/U_p = 1$) is underestimated by the k-ϵ model prediction

6) The calculations show that the inlet profiles of k and e have strong influence on the flow field of a confined jet without swirl. The effects of inlet boundary conditions extend to the further downstream of the reattachment region.

7) The influence of the inlet turbulence level in the confined coaxial swirling jet is less important compared to the non-swirling case. The influence is only appreciable in the initial region of the flow and has no significant effect in the downstream region.

8) The k-ϵ model failed to predict the momentum transport for swirling flows with intermediate swirl number   Higher order turbulence models which take into account the anisotropic turbulent viscosity effects are necessary for the swirling flow field predictions,

9) The k-e model prediction of PHOENICS and TEACH codes exhibit some qualitative discrepancies in the predicted results when compared to the measurements. These codes may have to be modified to improve the predictions.

POSTSCRIPT

Subsequent to the completion of this study, it was found that the qualitative difference on the predictions of the kinetic energy profiles discussed in Section IV was caused by the different averagmg processes [c.f. Ref 10, p. 45] employed by the two computer codes. TEACH code uses arithmatic averagmg while PHOENICS code utilizes harmonic averaging processes. Using an arithmatic averaging process, PHOENICS code produces kinetic energy contours and velocity profiles similar to those of the TEACH code. However, the long tail of the recirculation region observed when using PHOENICS code still persists. The tail region is probably caused by the different implementation of the wall functions.

According to Patankar [101, in the vicinity of wall region a rather fine grid, which was used in this study, would reduce the difference between the two averaging processes. The drastic difference of the kinetic energy contours produced by the two averaging processes near the wall region (as discussed in Section IV) definitely needs further investigation.

REFERENCES

1   Pope, S. B.   An Explanation of the Turbulent Round Jet/Plane Jet Anomaly.   AIAA J , Vol. 16, 1978, pp. 279-281

2.   Wood, P E. and Chen, C. P   Turbulence Model Predictions of the Radial Jet – A Comparison of **k-e** Models. Can, J Ch. E., Vol. 63, 1985, pp 177-182

3.   Nallasamy, M   A Critical Evaluation of Various Turbulence Models as Applied to Internal Fluid Flows. NASA Technical Paper 2474, 1985

4.   Sturgess, G. J., Syed, S. A., and McManus, K. R   Importance of Inlet Boundary Conditions for Numerical Simulation of Combustor Flows, AIAA paper No. Al AA-83-1263,

5   Ramos, J I.   Turbulent Nonreaching Swirling Flows. AIAA J., Vol. 22, 1983, pp. 846-848.

6.   Leschziner, M. A. and Rodi, W   Computation of Strongly Swirling Axisymmetric Free Jets. AIAA J., Vol. 22, 1984, pp. 1742-1747.

7   Launder, B., Morse, A., Rodi, W., and Spalding, D. B   Prediction of Free Shear Flows – A Comparison of the Performance of Six Turbulence Models. NASA SP-321, 1973.

8.   Spalding, D. B.   A General Purpose Computer Program for Multidimensional One and Two Phase Flow   Mathematics and Computers in Simulation, Vol. XXIII, North Holland Press, 1981, pp. 267-276.

9.   Gosman. A. D. and Pun, W M   Calculation of Recirculating Flows. Dept. No. HTS/74/12, 1974, Dept, of Mechanical Engineering, Imperial College, London, England.

10. Patankar, S. V   Numerical Heat Transfer and Fluid Flow. Hemisphere, 1980.

11   Kim, J., Kline S. and Johnston, J   Investigation of Separation and Reattachment of a Turbulent Shear Layer. Flow over a Backward Facing Step. Report MD, 37, Mech. Engr, Stanford University

12. Chaturvedi, M. C.   Flow Characteristids of Axisymmetric Expansion. J Hydraulics Div., Proc. ASCE, Vol. 89, No. Hy3, 1963.

13   Moon, L. F and Rudinger, G.   Velocity Distribution in an Abruptly Expanding Circular Duct. J Fluids Engr., Vol. 99, 1977, pp. 225-230.

14. Pope, S. B. and Whitelaw, J H.   The Calculation of Near Wake Flows. J. Fluid Mech., Vol. 73, 1976, pp. 9-32.

15. Qin, H.   The Flow Characteristics **of** a Sudden Axisymmetric Expansion. PDR/CRDU IC/4, Imperial College, London, 1984.

16. Launder, B. E.   1981-Stanford Conference on Complex Turbulent Flows, Computation and Experiment, Vol. II, pp. 843-862.

17   Johnston, J P   Internal Flows in Turbulence. Edited by P Bradshaw, Springer-Verlag, 1978

18.   Westphal, R. V and Johnston, J P   Effect of Initial Conditions on Turbulent Reattachment Downstream of a Backward Facing Step. AIAA J., Vol. 12, 1984, pp. 1227-1232.

19   Habib, M A. and Whitelaw, J. H.   Velocity Characteristics of a Confined Coaxial Jets. J Fluid Eng., Vol. 101, 1979, pp. 521-529.

20.   Johnson, B. V and Bennett, J C.   Mass and Momentum Turbulent Transport Experiments with Confined Coaxial Jets. NASA CR-165574, 1981.

21   Owen, F K.   Measurements and Observations of Turbulent Recirculating Jet Flows. AIAA J., Vol. 14, 1976, pp. 1556-1562.

22.   Ramos, J I.   Numerical Solution of Non-Premixed Reactive Flows in a Swirl Combustor Model. Eng. Comput., Vol. 1, 1984, pp. 173-182.

23   Schlichting, J H   Boundary Layer Theory. McGraw Hill, New York, NY, 1968.

24.   Gupta, A K., Lilley, D G and Syred, N.   Swirl Flows. Abacus Press, 1984.

25   Habib, M A and Whitelaw, J H.   Velocity Characteristics of Confined Coaxial Jets With and Without Swirk. J Fluids Eng., Vol. 102, pp. 47-53.

26.   Roback, R. and Johnson, B. V   Mass and Momentum Turbulent Transport Experiments with Confined Swirling Coaxial Jets. NASA CR-168252, 1983,

27   Sturgess, G. J   Aerothermal Modeling Phase 1. NASA CR-168202, 1983

28.   Rodi, W   Influence of Buoyancy and Rotations on Equations for the Turbulent Length Scale. Proc. of Turb. Shear Flows 2, Imperial College, London, 1979, pp. 10.37-10.42.

29   Gosman, A. D., Khalil, E. E., and Whitelaw, J H   The calculation of Two-Dimensional Turbulent Recirculating Flows. Turbulent Shear Flows, Vol. 1, 1979, pp. 237-255.

30.   Driver, D. M and Seagmiller Features of a Reattaching Turbulent Shear Layer in Divergent Channel Flow   AIAA J., Vol. 23; 1985, pp. 163-171.

31   Hinze, J O. Turbulence. McGraw-Hill, New York, NY, 1975.

1. REPORT NO. NASA CR-3929	2. GOVERNMENT ACCESSION NO.	3. RECIPIENT'S CATALOG NO.
4. TITLE AND SUBTITLE Studies on Effects of Boundary Conditions in Confined Turbulent Flow Predictions		5. REPORT DATE September 1985
		6. PERFORMING ORGANIZATION CODE
7. AUTHOR(S) M. Nallasamy and C. P. Chen *		8. PERFORMING ORGANIZATION REPORT #
9. PERFORMING ORGANIZATION NAME AND ADDRESS Universities Space Research Association The American City Building, Suite 311 Columbia, MD 21044		10. WORK UNIT NO. M-499
		11. CONTRACT OR GRANT NO. NAS8-35918
12. SPONSORING AGENCY NAME AND ADDRESS National Aeronautics and Space Administration Washington, D.C. 20546		13. TYPE OF REPORT & PERIOD COVERED Contractor Report
		SPONSORING AGENCY CODE

15. SUPPLEMENTARY NOTES *National Research Council Research Associate
Prepared for the Fluid Dynamics Branch, Atmospheric Sciences Division, Systems Dynamics Laboratory, Science & Engineering Directorate. Contract Monitor: N. C. Costes

16. ABSTRACT

This report investigates the differences in k-ε model predictions of plane and axisymmetric expansion flows. The prediction of the coaxial jet for different velocity ratios of the annular to central jet is presented. The effects of inlet kinetic energy and the energy dissipation rate profiles are investigated for swirling and nonswirling flows. The effects of expansion ration and Reynolds number on the reattachment length are also presented. The results show that the inlet k and E profiles have the most significant effect on the reattachment length and flow redevelopment for the case of aoaxial jet of high velocity ratio.

A comparison of k-ε model predictions for the pipe expansion flow by the PHOENICS and TEACH codes reveals some discrepancies in the predicted results. TEACH prediction seems to produce unrealistic kinetic energy profiles in some regions of the flow. PHOENICS code produces a long tail in the recirculation region under certain conditions.

17. KEY WORDS Computational Fluid Dynamics Turbulent Flow Turbulence Models Internal Flow	18. DISTRIBUTION STATEMENT Unclassified–Unlimited Subject Category: 34

19. SECURITY CLASSIF. (of this report) Unclassified	20. SECURITY CLASSIF. (of this page) Unclassified	21. NO. OF PAGES 36	22. PRICE A03